

Journal Pre-proof

Thiazolidine-2,4-dione-based irreversible allosteric IKK- β kinase inhibitors:
Optimization into *in vivo* active anti-inflammatory agents

Ahmed Elkamhawy, Nam youn Kim, Ahmed H.E. Hassan, Jung-eun Park, Sora Paik,
Jeong-Eun Yang, Kwang-Seok Oh, Byung Ho Lee, Mi Young Lee, Kye Jung Shin, Ae
Nim Pae, Kyung-Tae Lee, Eun Joo Roh

PII: S0223-5234(19)31107-9

DOI: <https://doi.org/10.1016/j.ejmech.2019.111955>

Reference: EJMECH 111955

To appear in: *European Journal of Medicinal Chemistry*

Received Date: 6 August 2019

Revised Date: 5 December 2019

Accepted Date: 5 December 2019

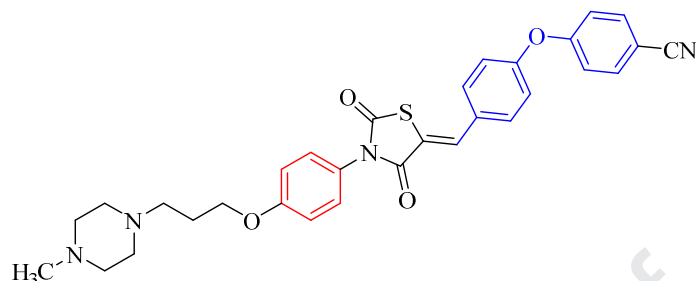
Please cite this article as: A. Elkamhawy, N.y. Kim, A.H.E. Hassan, J.-e. Park, S. Paik, J.-E. Yang, K.-S. Oh, B.H. Lee, M.Y. Lee, K.J. Shin, A.N. Pae, K.-T. Lee, E.J. Roh, Thiazolidine-2,4-dione-based irreversible allosteric IKK- β kinase inhibitors: Optimization into *in vivo* active anti-inflammatory agents, *European Journal of Medicinal Chemistry* (2020), doi: <https://doi.org/10.1016/j.ejmech.2019.111955>.

This is a PDF file of an article that has undergone enhancements after acceptance, such as the addition of a cover page and metadata, and formatting for readability, but it is not yet the definitive version of record. This version will undergo additional copyediting, typesetting and review before it is published in its final form, but we are providing this version to give early visibility of the article. Please note that, during the production process, errors may be discovered which could affect the content, and all legal disclaimers that apply to the journal pertain.

© 2019 Published by Elsevier Masson SAS.



Graphical Abstract

**7a**

Irreversible allosteric IKK- β inhibitor

$$IC_{50} = 200 \text{ nM}$$

$$K_{\text{inact}} = 0.013 \text{ min}^{-1}$$

$$\text{TNF-}\alpha \text{ IC}_{50} = 6.27 \text{ }\mu\text{M}$$

$$\text{PGE}_2 \text{ IC}_{50} = 9.83 \text{ }\mu\text{M}$$

Plasma stability = 73.6% after two hours

Microsomal stability $t_{1/2}$ = 1 hour

In vivo protection against septic shock = 80% survival at 36 hours post injection

Thiazolidine-2,4-dione-based irreversible allosteric IKK- β kinase inhibitors:

Optimization into *in vivo* active anti-inflammatory agents

Ahmed Elkamhawy^{a,b,1}, Nam youn Kim^{a,1}, Ahmed H.E. Hassan^{c,1}, Jung-eun Park^a, Sora Paik^{a,d}, Jeong-Eun Yang^a, Kwang-Seok Oh^e, Byung Ho Lee^e, Mi Young Lee^e, Kye Jung Shin^f, Ae Nim Pae^{g,h}, Kyung-Tae Leeⁱ, Eun Joo Roh^{a,h*}

^a Chemical Kinomics Research Center, Korea Institute of Science and Technology (KIST), Seoul 02792, Republic of Korea.

^b Department of Pharmaceutical Organic Chemistry, Faculty of Pharmacy, Mansoura University, Mansoura 35516, Egypt.

^c Department of Medicinal Chemistry, Faculty of Pharmacy, Mansoura University, Mansoura 35516, Egypt.

^d Department of Fundamental Pharmaceutical Sciences, College of Pharmacy, Kyung Hee University, Seoul, 02447, Republic of Korea.

^e Therapeutics & Biotechnology Division, Korea Research Institute of Chemical Technology, 141 Gajeong-ro, Yuseong, Daejeon 34114, Republic of Korea.

^f Integrated Research Institute of Pharmaceutical Sciences, College of Pharmacy, The Catholic University of Korea, Bucheon-si, Gyeonggi-do 14662, Republic of Korea.

^g Convergence Research Center for Diagnosis, Treatment and Care System of Dementia, Korea Institute of Science and Technology (KIST), Seoul 02792, Republic of Korea.

^h Division of Bio-Medical Science & Technology, KIST School, Korea University of Science and Technology, Seoul 02792, Republic of Korea

ⁱ Department of Life and Nanopharmaceutical Sciences, Kyung Hee University, Seoul 02447, Republic of Korea.

¹ These authors contributed equally to this work

*Corresponding author:

Eun Joo Roh: r8636@kist.re.kr

Abstract

Selective kinase inhibitors development is a cumbersome task because of ATP binding sites similarities across kinases. On contrast, irreversible allosteric covalent inhibition offers opportunity to develop novel selective kinase inhibitors. Previously, we reported thiazolidine-2,4-dione lead compounds eliciting *in vitro* irreversible allosteric inhibition of IKK- β . Herein, we address optimization into *in vivo* active anti-inflammatory agents. We successfully developed potent IKK- β inhibitors with the most potent compound eliciting $IC_{50} = 0.20 \mu M$. Cellular assay of a set of active compounds using bacterial endotoxin lipopolysaccharide (LPS)-stimulated macrophages elucidated significant *in vitro* anti-inflammatory activity. *In vitro* evaluation of microsomal and plasma stabilities showed that the promising compound **7a** is more stable than compound **7p**. Finally, *in vivo* evaluation of **7a**, which has been conducted in a model of LPS-induced septic shock in mice, showed its ability to protect mice against septic shock induced mortality. Accordingly, this study presents compound **7a** as a novel potential irreversible allosteric covalent inhibitor of IKK- β with verified *in vitro* and *in vivo* anti-inflammatory activity.

Keywords:

IKK- β modulators; NF- κ B signaling pathway; Thiazolidine-2,4-diones; Allosteric modulation; Anti-inflammatory.

1. Introduction

Encompassing more than five hundred members, kinases are the third largest class of enzymes [1]. More than 30% of the entire set of proteins expressed in humans estimated to undergo phosphorylation kinases [2]. Irregular hyperactivity of certain kinases has been characterized in some pathological conditions including tumors, neurological and inflammatory diseases. Therefore, development of the specific kinase inhibitors has become a hot topic in drug discovery programs [3-8]. As most of the devoted efforts have focused on targeting the ATP binding pocket, which bears similarities across different kinases, development of a selective inhibitor is a challenge. Poorly selective ATP competitive molecules could face limited clinical application [9]. Lately, development of allosteric kinase modulators gained traction among researchers in the field as targeting the more variable sites of kinases might afford more efficiently selective ligands [10-12]. Also recently, more evidences have accumulated documenting the possibility of developing covalent inhibitors that could be more efficient than the classical reversible inhibitors, yet, are devoid from the previously doubted toxicities [13-18]. In fact, the concept of covalent inhibition has been extended to the development of covalent allosteric inhibitors that has been claimed to offer higher level of selectivity and potency [19-21].

The “nuclear factor kappa-light-chain-enhancer of activated B cells” (NF- κ B) is a transcription factor that induces the expression of more than 500 genes encompassing several pro-inflammatory genes, including cytokines (TNF- α , IL-1 β and IL-6), chemokines (CCL5, CCL20, CXCL8 and CXCL10) in addition to proinflammatory enzymes including inducible nitric oxide synthase (iNOS) and cyclooxygenase-2 (COX2) [5, 22-25]. In addition, NF- κ B-triggered genes expression invokes immunological responses, cells proliferation, and apoptosis [26, 27]. The canonical NF- κ B signaling pathway is activated by the kinase IKK- β

(inhibitor of nuclear factor kappa-B kinase subunit beta) which phosphorylates I κ B (inhibitor of NF- κ B) resulting in release and translocation of NF- κ B into the nucleus [28]. Because IKK- β is a bottleneck for activation of NF- κ B signaling pathway, its inhibition might be a successful strategy for treatment of acute and chronic inflammatory diseases, as well as, cancer and autoimmune diseases [28-31]. In addition to I κ B, IKK- β phosphorylates other substrates such as TSC1, SNAP23 and Foxo3a [32, 33]. Consequently, it elicits NF- κ B-independent signals in inflammation mediated tumor angiogenesis, mast cell degranulation and cell cycle arrest [34-36].

Several literatures report development of inhibitors of NF- κ B signaling pathway including IKK- β inhibitors of diverse chemical scaffolds [26, 31]. As far as we know, most of the developed IKK- β inhibitors are reversible competitive inhibitors; for example, compound **1** (Fig. 1) developed by the Bayer pharmaceutical company [37]. Although irreversible allosteric inhibitors offer advantages over the reversible classical ATP competitive inhibitors as mentioned previously, reports of even reversible allosteric IKK- β inhibitors are limited (e.g. BMS-345541 (**2**); a non-selective allosteric inhibitor of both IKK- α and IKK- β [24]). There is an obvious need to develop small molecules as covalent allosteric inhibitors of IKK- β . A recent report revealed that the natural product (+)-ainsliadimer (**3**) covalently inhibits IKK- β at an allosteric site [38]. In another report, covalent binding of the natural product isoliquiritigenin (**4**) was also found to suppress the activity of T lymphocytes [39]. Recently, Park *et al.* reported 1,3,5-triazine-2,4-diamine derivative (**5**) as an IKK- β inhibitor hit compound and used it as starting point to develop orthosteric IKK- β inhibitors [40]. Their report presented also a 2-imino-4-thiazolidin-4-one derivative as a hit compound possessing high IC₅₀ value of 97.4 μ M. In a recent report, we have undertaken the task of development of the latter hit compound into thiazolidine-2,4-dione derivative **6** which elicited a potential

in vitro covalent allosteric inhibition of IKK- β but still its IC₅₀ value is in the micromolar range [41]. Despite further attempt to optimize the kinase inhibitory activity, the latter compounds were not advanced for further cell-based or *in vivo* evaluation [42]. In this report, we address optimization of the lead compound **6** into more potent irreversible allosteric IKK- β inhibitor with potential *in vivo* anti-inflammatory activity.

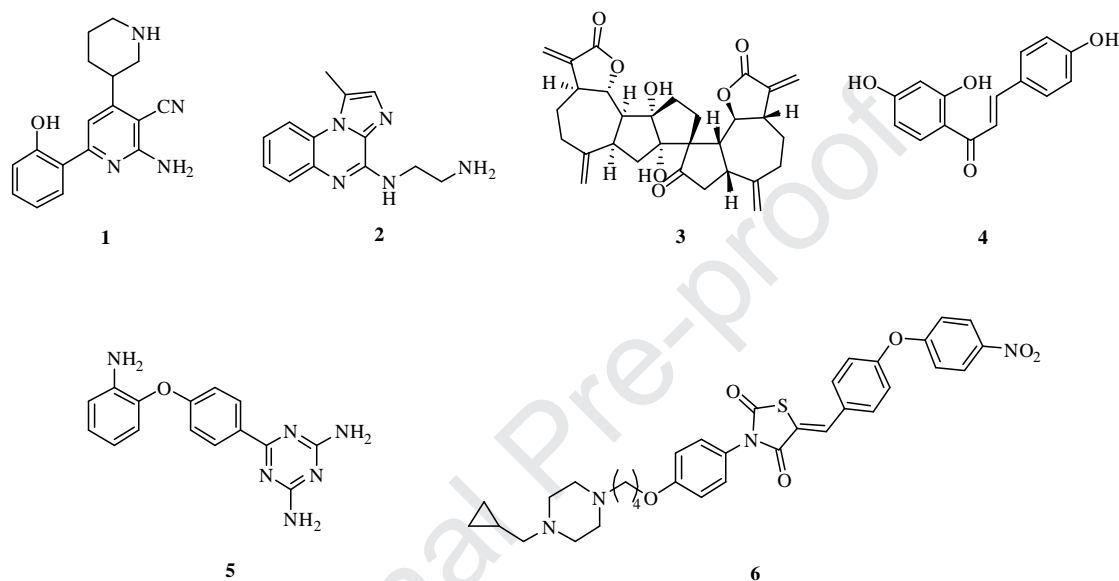


Fig. 1. Reported inhibitors compounds for IKK- β

In this study, as shown in Fig. 2, we explored variable lengths of the alkyloxy chain linker in addition to studying the outcome of variation of the linker attachment point between *para* and *meta* positions of the phenyl ring attached to the nitrogen atom of the thiazolidine-2,4-dione scaffold. Congruent with reported influence of cycloalkylamines modification such as piperazines on bioactivity [43], we found in our previous report that the terminal *N*-substituent on piperazine ring elicits a crucial impact on the elicited activity with the all carbon substituents, such as *N*-cyclopropylmethyl, eliciting higher activity than *N*-substituents possessing the more polar oxygen or sulfur atom. We fixed this terminal *N*-substituent to methyl, which is a one-carbon substituent. Since the structure of IKK- β

incorporates an important cysteine residue (Cys46) which exists in the vicinity of an allosteric site located close to the catalytic ATP pocket (protein databank code: 3QA8) [44], the observed irreversible allosteric inhibition might result from Michael addition of thiol group to the double bond of the benzylidene moiety of compound **6**. Because variable substituents attached to the benzylidene moiety might elicit different electron push-pull, which would affect the Michael addition of thiol group of cysteine, we prepared compounds **7** possessing variable substituents on the phenoxy ring attached to the benzylidene moiety. Accordingly, we would like to report our promising results.

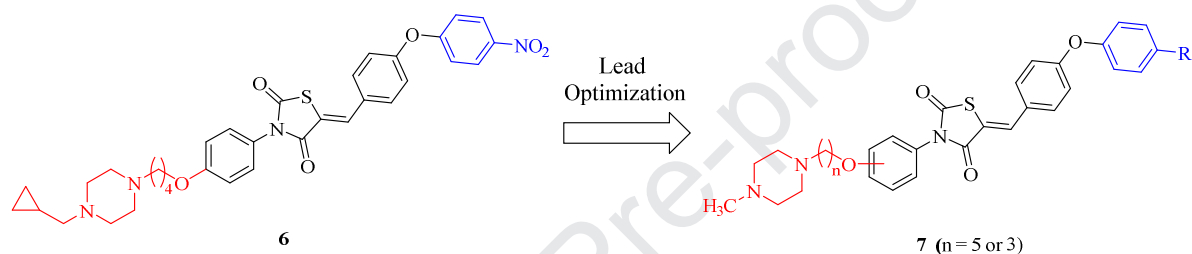


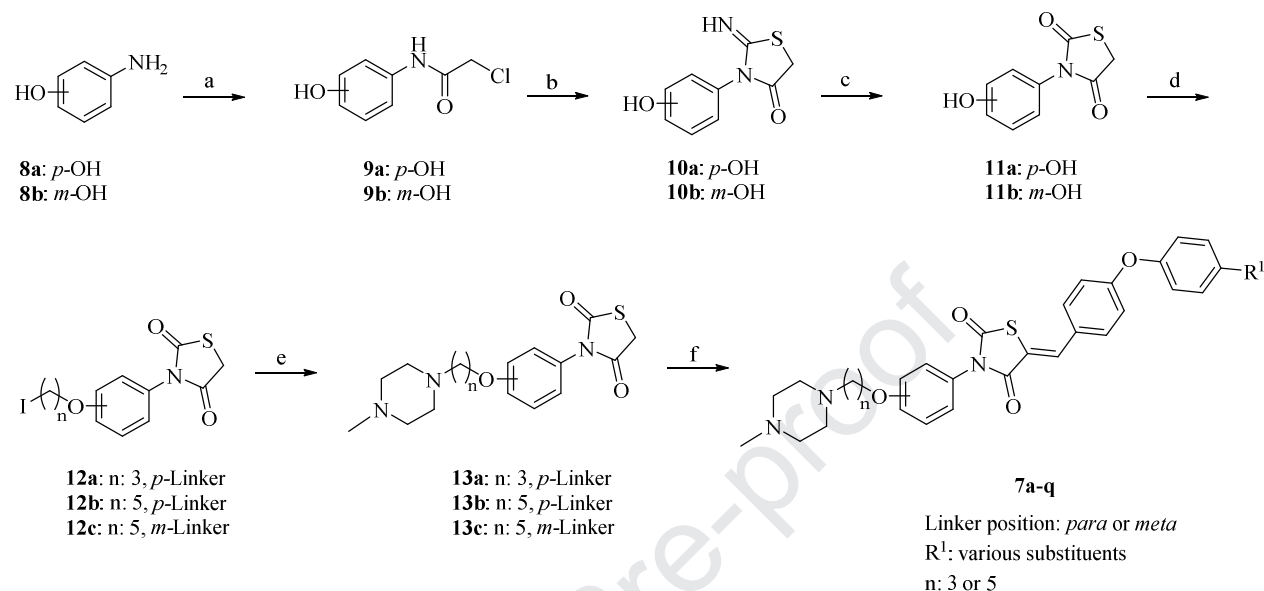
Fig. 2. Design of the novel thiazolidine-2,4-dione derivatives (**7**)

2. Results and discussion

2.1. Chemistry

As illustrated in Scheme 1, a straightforward synthesis of the target compounds (**7**) was performed in six steps starting from 4-aminophenol (**8a**) or 3-aminophenol (**8b**). Thus, amide coupling with chloroacetyl chloride yielded acetamide derivatives **9**. Nucleophilic displacement of chlorine atom of acetamide derivatives **9** with thiocyanate followed by cyclization afforded the 2-iminothiazolidin-4-one derivatives **10** [45]. Acidic hydrolysis afforded the desired thiazolidine-2,4-dione intermediates **11** [46]. *O*-Alkylation of the phenolic hydroxyl group with 1,*n*-diiodoalkanes allowed installation of alkyl chain linker to yield derivatives **12**. *N*-Alkylation of 1-methylpiperazine with the prepared derivatives **12** provided the corresponding thiazolidine-2,4-dione derivatives **13**. Lastly, Knoevenagel

condensation with various benzaldehyde derivatives afforded the designed compounds (7, Table 1) [47].



Scheme 1. Reagents and reaction conditions: (a) chloroacetyl chloride, DCM, 0 °C, 1.5 h, rt, 3 h; (b) KSCN, acetone, 65 °C, 7 h; (c) 2% HCl aqueous solution, 100 °C, 7 h; (d) diiodoalkane, K₂CO₃, MeCN, 95 °C, 7 h; (e) 1-methylpiperazine, K₂CO₃, MeCN, rt, 9 h; (f) appropriate aldehyde derivative, NaOAc, AcOH, 110 °C, 16 h.

2.2. Biological evaluation

2.2.1. *In vitro* IKK-β induced phosphorylation modulation

As previously mentioned, all of the designed, synthesized and evaluated final compounds have *m*- or *p*-hydroxyphenyl moiety at 3-position of the thiazolidine-2,4-dione scaffold. The hydroxyphenyl moiety is *O*-alkylated with an alkyl chain tether to link it to *N*-methylpiperazine moiety. The alkyl linker was varied in length (*n* = 3 or 5) while the introduced substituents on the phenoxyphenyl moiety attached to the 5-exomethylene group on the thiazolidine-2,4-dione ring have variable electronic characters as shown in Table 1. *In vitro* evaluation of the IKK-β inhibitory activity of the synthesized 17 final compounds were performed employing a 5-FAM (5-carboxyfluorescein) labeled IκBα-derived polypeptide (5-

FAMGRHDSGLDSMK-NH₂; R7574, MDS Analytical Technologies) as a substrate for IKK- β in an IMAP[®] based fluorescence assay [48]. To secure high sensitivity and accuracy for the conducted *in vitro* assay, it was carried out as time-resolved Förster resonance energy transfer assay (TR-FRET assay) [49]. As the percent inhibition and IC₅₀ of irreversible inhibitors increase by time, the measurements were recorded after two hours of interaction of 10 μ M concentrations of the tested compound with IKK- β to permit the inactivation reaction to approach completion.

Table 1. Results of IKK- β assay using the synthesized new ligands (**7a–7q**).

Cpd	n	Linker Position	R ¹	IKK- β assay IC ₅₀ (μ M) ^a	Cpd	n	Linker Position	R ¹	IKK- β assay IC ₅₀ (μ M) ^a
7a	3	<i>p</i>	CN	0.20	7j	5	<i>m</i>	F	6.06
7b	3	<i>p</i>	F	0.67	7k	5	<i>m</i>	Cl	2.61
7c	5	<i>p</i>	F	0.60	7l	5	<i>m</i>	Br	2.67
7d	5	<i>p</i>	Cl	0.70	7m	5	<i>m</i>	CH ₃	2.73
7e	5	<i>p</i>	Br	0.43	7n	5	<i>m</i>	OCH ₃	2.43
7f	5	<i>p</i>	OCH ₃	0.70	7o	5	<i>m</i>	NH ₂	8.07
7g	5	<i>p</i>	CH ₃	0.87	7p	5	<i>m</i>	NO ₂	0.22
7h	5	<i>p</i>	NH ₂	2.61	7q	5	<i>m</i>	CN	0.84
7i	5	<i>p</i>	NHCOCH ₃	1.71					

^a IC₅₀ values (μ M) exhibited by the newly synthesized compounds

As shown in Table 1, we first explored the biological activity of compounds whose linkers were attached to the *para* position. Analogs **7a** and **7b** possessing the three carbons linker were significantly active molecules. While compound **7b** possessing the electronically amphiphilic 4-fluoro substituent elicited an excellent submicromolar IC₅₀ of 0.67 μ M, compound **7a** possessing the electronegative 4-cyano group was more potent eliciting IC₅₀ of 0.20 μ M. Extending the length of the alkyl chain linker of compound **7b** by two carbons provided compound **7c** with almost similar potency (Table 1). While variation of the substituent to include the electronically amphiphilic 4-bromo substituent in derivative **7e**

resulted in more potent compound than derivatives **7f** and **7g** which have the electron donating 4-methoxy or 4-methyl moieties, compound **7d** possessing 4-chloro substituent elicited similar potency to compound **7f**. However, more decrement of the potency was elicited in derivatives **7h** and **7i** possessing the electron donating 4-amino or 4-acetamido moieties, respectively. With IC_{50} value of 0.43 μM , the 4-bromo derivative **7e** was the most potent among compounds possessing a linker of 5 carbon atoms, however, it has the double IC_{50} of compound **7a** possessing 3 carbon atoms linker.

Next, we explored the outcome of displacing the linker from *para* to *meta* position via preparation and evaluation of compounds **7j–q**. Comparing the activities of *meta* and *para* linked compounds possessing the same substituent on exomethylene moiety unveiled an interesting activity trend. As Table 1 illustrates, derivative **7o** possessing 4-amino moiety showed relatively higher micromolar IC_{50} value of 8.07 μM while the corresponding derivative **7h** with *para* attached linker showed IC_{50} value of 2.61 μM , which was the least potent among those compounds possessing the *para* attached linker. In addition, displacement of the linker's attachment point to *meta* position in compounds **7j**, **7k** and **7l**, possessing the electronically amphiphilic 4-halo substituents resulted in much less potent than the corresponding derivatives having the linker attached to the *para* position. Thus, compounds **7j**, **7k**, **7l**, **7m** and **7n** elicited micromolar IC_{50} values ranging between 2.61 to 6.06 μM . Similarly, the *meta*-attached linker compounds **7m** and **7n** having the electron donating 4-methyl and 4-methoxy, respectively, were less potent relative to the corresponding compounds **7f** and **7g** possessing the *para*-attached linker. Thus, as shown in Table 1, compounds **7m** and **7n** possessed micromolar IC_{50} values in comparison with the submicromolar IC_{50} values of compounds **7f** and **7g**. On the other hand, replacement of the electronically amphiphilic 4-halo; the electron donating 4-methoxy, 4-methyl and 4-amino

moieties with the electron withdrawing 4-nitro or 4-cyano yielded the potent compounds **7p** and **7q** showing submicromolar IC_{50} values. In conclusion, these results suggest that attaching the linker to the *para* position might generally be more favorable than attaching it to the *meta* position. In addition, compounds bearing electron withdrawing substituents might be more active than those with electron donating or amphiphilic substituents.

2.2.2. Mechanistic study of the induced IKK- β inhibition

Since we expect that these compounds to bind covalently to IKK- β , we selected the most active inhibitors, as revealed in the biological assay against IKK- β , for investigation of the elicited mode of IKK- β inhibition. Accordingly, the kinetic dose-response curves (measurement intervals equivalent to 0, 20, 40 and 60 min) were generated using approximately three-fold dilutions (30, 10, 3, 1, 0.3, 0.1, 0.03, 0.01, 0.003 and 0.001 μ M) for each of compounds **7a** and **7p** (Fig. 3). First, the validity of data was verified by calculating the standard errors for tops, bottoms, HillSlope, spanning values for the curves and checking the goodness of fitting; all of which showed excellent values and 95% confidence spanning nearly the measured ranges. The kinetic measurements showed that increasing the time boosts the elicited inhibitions; a characteristic of irreversible inhibition reaction. Table 2 summarizes the parameters of kinetic dose response curves. At zero time, the maximum inhibition elicited by compound **7a** was 60.9% but increased to 76.6% after 60 min. In contrast, compound **7p** was less effective at zero time showing a maximum inhibition of 53.2%, but after 60 min., it elicited a maximum inhibition percent of 89.2% rendering it was more effective by time than compound **7a**. The HillSlope of compound **7p** was higher than that of compound **7a** indicating higher rate of the irreversible inactivation reaction of IKK- β by compound **7p**. Considering the fact that interaction of irreversible inhibitors with the target protein involves an initial physical binding step followed by a second step of chemical

interaction to establish a covalent bond, these kinetic data might indicate compound **7a** possessing the *para* attached linker elicits a better physical binding phase but a lower rate of chemical interaction relative to compound **7p**. Following the published method for calculation of K_{inact} values [50], nonlinear regression after calculating the K_{obs} for each concentration of compounds **7a** and **7p** returned K_{inact} values of 0.013 and 0.027 (min^{-1}), respectively.

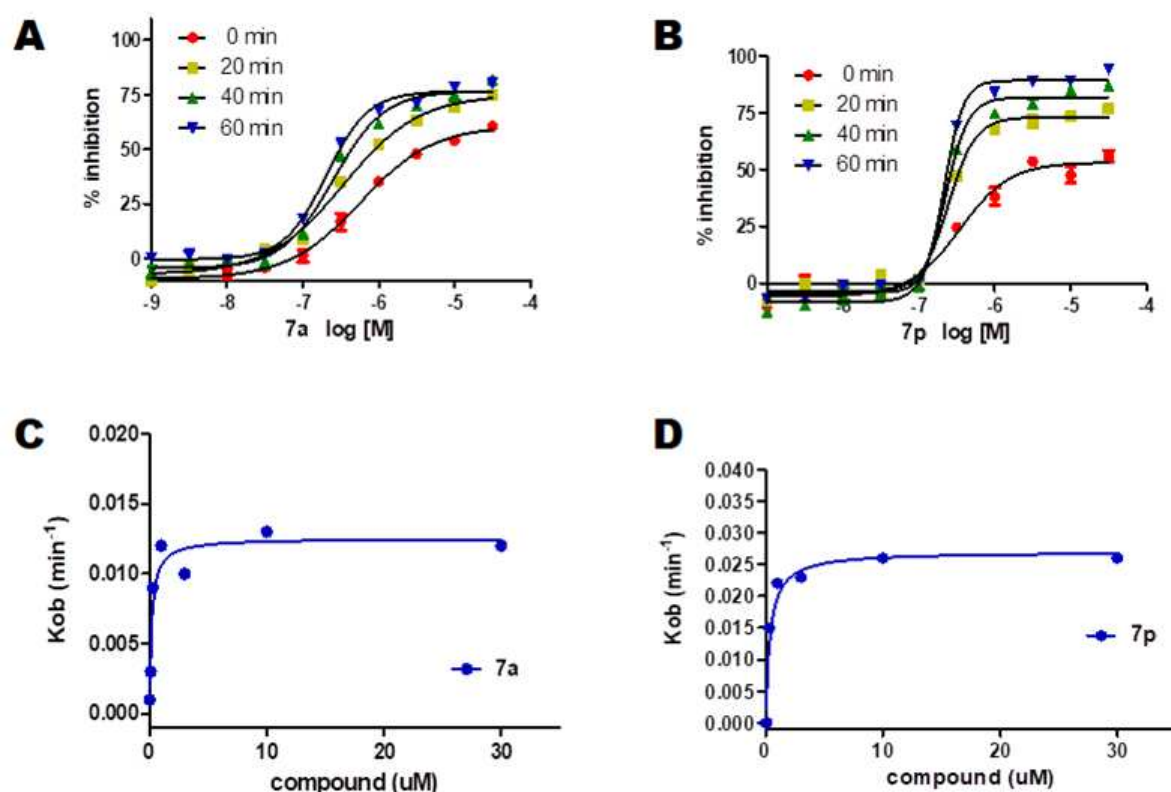


Fig. 3. A) Time-dependent dose-responses curves of compound **7a**. B) Time-dependent dose-responses curves of compound **7p**. C) Nonlinear regression of calculated K_{obs} values against concentration of compound **7a**. D) Nonlinear regression of calculated K_{obs} values against concentration of compound **7p**.

Table 2. Parameters of the time-dependent dose response curves for inhibition of IKK- β by compounds **7a** and **7p** measured by TR-FRET assay

Compound	7a				7p				
Time intervals	0 min	20 min	40 min	60 min	0 min	20 min	40 min	60 min	
Best-fit values	Bottom	-9.33	-7.14	-4.47	-0.38	-5.63	-3.68	-8.33	-3.88
	Top	60.9	75	76.7	76.6	53.2	73	81.8	89.2
	-LogIC ₅₀	-6.24	-6.46	-6.6	-6.69	-6.46	-6.61	-6.66	-6.66
	HillSlope	0.9	0.87	1.29	1.56	1.32	2.43	2.8	3.47
	Span	70.2	82.1	81.2	77	58.8	76.7	90.1	93.1

	Bottom	1.29	1.54	1.65	1.21	1.81	1.33	1.48	1.11
	Top	2.21	2.09	1.85	1.25	2.27	1.38	1.49	1.12
Std. Error	LogIC ₅₀	0.05	0.05	0.04	0.03	0.07	0.03	0.03	0.02
	HillSlope	0.09	0.08	0.15	0.15	0.25	0.36	0.37	0.41
	Span	2.89	2.99	2.68	1.84	3.14	1.98	2.14	1.6
95% Confidence Intervals	Span	64.23 ~ 76.12	75.99 ~ 88.26	75.68 ~ 86.70	73.18 ~ 80.75	52.33 ~ 65.23	72.58 ~ 80.72	85.75 ~ 94.54	89.77 ~ 96.33
Goodness of Fit	DF ^a	26	26	26	26	26	26	26	26
	R ²	0.99	0.99	0.98	0.99	0.96	0.99	0.99	0.99

^a DF: Degrees of Freedom

2.2.3. Cellular assays for anti-inflammatory activity

As kinase assays showed a potential *in vitro* IKK- β inhibitory activity, a cellular level biological investigation for a set of active derivatives on the viability and inflammatory mediators has been explored. Among several biological responses stimulated by LPS in RAW 264.7 macrophages, the NF- κ B signaling pathway is upregulated resulting in overproduction of pro-inflammatory cytokines (TNF- α , IL-6) and nitric oxide [51, 52]. Therefore, the production of these inflammatory mediators, as well as, the cell viability in LPS-treated RAW 264.7 macrophages were measured in presence of three doses (0.1, 1 and 10 μ M) of compounds **7a**, **7j**, **7k** and **7p**. The results are presented in the following sections.

2.2.3.1. Impact on RAW 264.7 macrophages Cells' Viability

Because induced macrophages' cells death, if any occurs, would lead to a reduction of the measured production of cytokines (TNF- α and IL-6) in addition to nitric oxide regardless the inhibition of IKK- β activity, cell viability assay was conducted to avoid inaccuracies arising from this factor. The assay was conducted at concentrations used for measurement of TNF- α , IL-6 and nitric oxide in presence and in absence of LPS. At 10 μ M concentration, as illustrated in Fig. 4, all of the tested compounds did not elicit cytotoxicity in absence of LPS.

Also in presence of LPS, compounds **7a**, **7k** and **7p** did not show significant cytotoxicity at the tested three concentrations. However, in presence of LPS, the 10 μM concentration of compound **7j** reduced the viability of macrophages eliciting IC_{80} value of 4.43 μM in presence of 1 $\mu\text{g/ml}$ of LPS (Table 3).

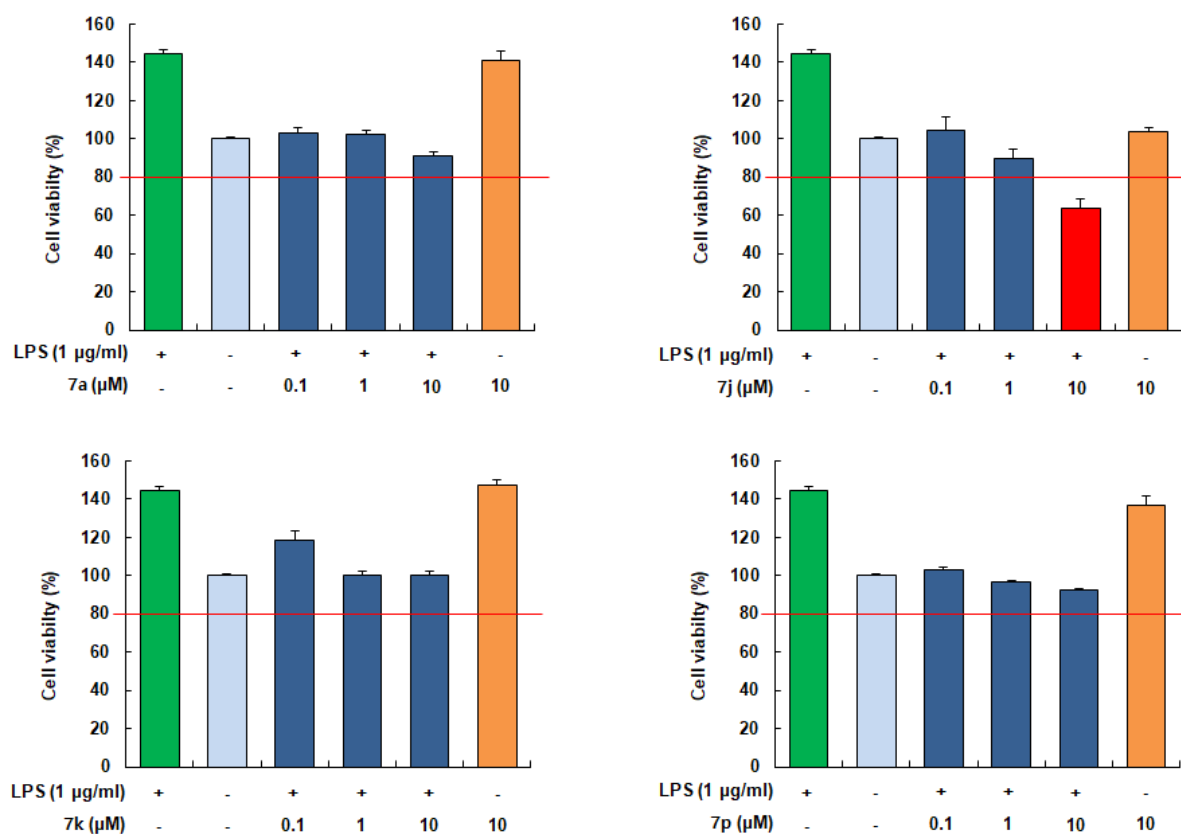


Fig. 4. Cell viability of RAW 264.7 macrophage cells: in absence of both of tested compound and LPS (cyan color), in presence of LPS (green color), in presence of 6 μM of tested compounds (dark buff color) and in presence of both of LPS and tested compounds (blue color). Red color indicates cytotoxicity of macrophages cells (viability percent below 80%).

Table 3. Viability of RAW 264.7 macrophages and IC_{50} for reduction of production of NO, IL-6 and $\text{TNF-}\alpha$.

Compound	IC_{80}^a (μM)		IC_{50}^b (μM)		
	Cell viability	$\text{TNF-}\alpha$	NO	PGE_2	IL-6
7a	>10	6.27	>10	9.83	>10
7j	4.43	7.87	>10	>10	>10
7k	>10	>10	>10	8.52	>10
7p	>10	5.22	>10	>10	>10

^a IC_{80} : defined as the concentration of the compound that decreases viability of cells to 80% in presence of 1

µg/ml of LPS.

^b IC₅₀: defined as the concentration that decreases the measured amount of produced TNF-α, NO, PGE₂ or IL-6 to 50%.

2.2.3.2. Effect on LPS-induced TNF-α production in RAW 264.7 macrophages

The production of the pro-inflammatory cytokine TNF-α is a downstream of several LPS-activated signaling pathways including NF-κB, MEK and ERK [53, 54]. Thus, inhibition of IKK-β as a limiting step in the canonical NF-κB signaling pathway would result in reduction of the inflammatory mediator TNF-α production levels. The results showed a dose dependent decrease of TNF-α production in presence of compound **7p** with 84% reduction relative to the amount produced by LPS (Fig. 5). Similarly, the 10 µM concentration of compounds **7a** and **7j** exerted reduction of LPS-stimulated TNF-α production by 80% and 71%, respectively. However, the 0.1 and 1 µM concentrations of both **7a** and **7j** did not result in a significant reduction. Lastly, compound **7k** was the least potent among evaluated compounds eliciting 44% reduction of TNF-α production at 10 µM concentration. The determined IC₅₀ values were 5.22, 6.27 and 7.87 for compounds **7p**, **7a** and **7j**, respectively (Table 3). These results indicate the anti-inflammatory properties of the prepared compounds.

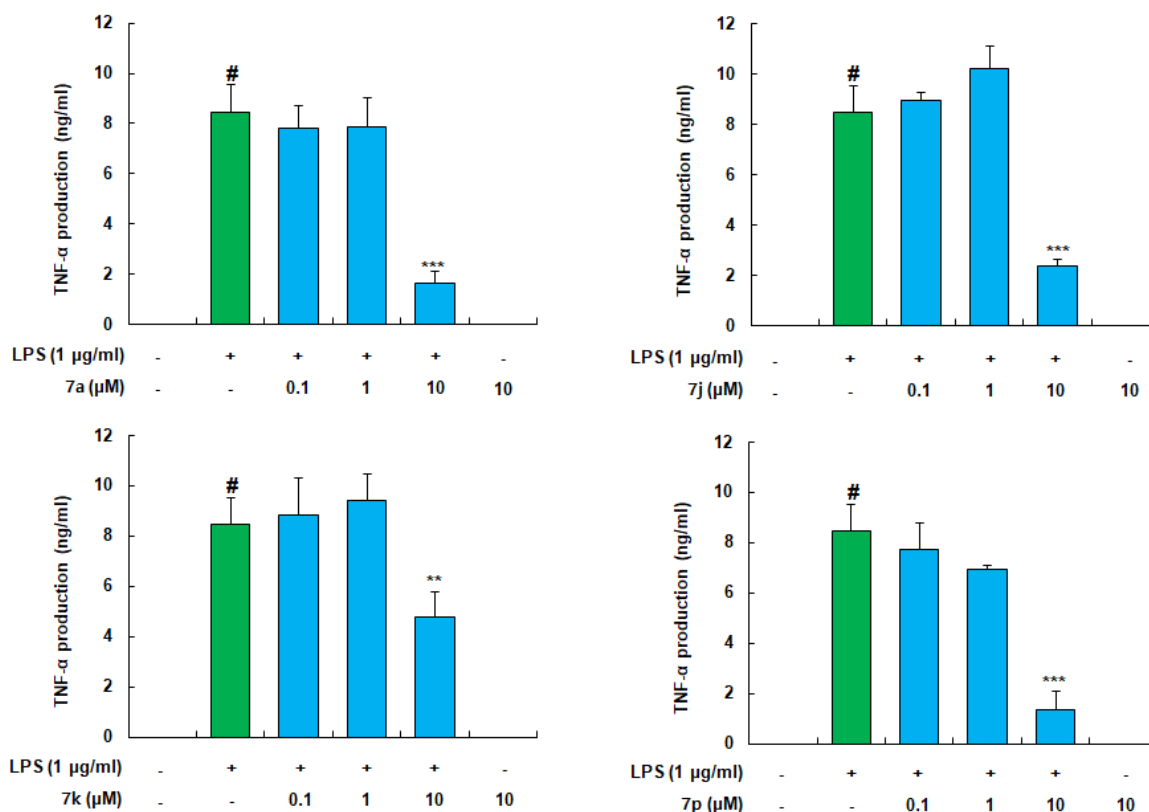


Fig. 5. Levels of TNF- α produced in RAW 264.7 macrophage cells; green color indicates presence of only LPS; blue color indicates presence of a candidate compound and LPS; ** $p < 0.01$, *** $p < 0.001$.

2.2.3.3. Effect on LPS-induced nitric oxide production in RAW 264.7 macrophages

Inducible nitric oxide synthase (iNOS) is responsible for production of nitric oxide in inflammatory conditions. The expression of iNOS is stimulated by several signaling pathways including NF- κ B, mitogen-activated protein kinases (p38, ERK1/2 and JNK) and JAK/STAT [5, 55]. Thus, inhibition of NF- κ B signaling pathway would result in reduction of nitric oxide (NO) production, at least in part. To determine the extent of contribution of the tested compounds to the reduction of NO production in LPS-stimulated RAW 264.7 macrophages, first, it was confirmed that the level of NO production in presence of 10 μ M concentration of only the candidate compound is unchanged from that of non-stimulated macrophages. Second, the amounts of NO produced in LPS-stimulated macrophages were measured in presence of increasing concentrations of tested compounds and referred to the amounts produced after and before LPS stimulation. A concentration of 40 μ M of the

selective inducible nitric oxide synthase inhibitor NIL was used as a standard for comparison [5, 25, 56]. As shown in Fig. 6, all of compounds **7j**, **7k** and **7p** showed a dose dependent significant reduction of NO production. Even though the low concentrations of compound **7a** did not elicit significant reduction of NO production, the 10 μ M concentration exerted significant reduction close to, albeit higher, the reduction of NO production by 40 μ M concentration of the standard NIL. Similarly, the 10 μ M concentration of compounds **7j** and **7k** elicited reduction of NO production approximating the reduction exhibited by 40 μ M concentration of the standard NIL. Even though compound **7p** was the least effective inhibitor of NO production, its ability was still significant at concentrations as low as 0.1 μ M. These data confirm the beneficial outcome of these compounds on reduction of NO production through blocking the NF- κ B signaling pathway. However, the measured high IC₅₀ values might be due to presence of other LPS-activated signaling pathways which also contribute to NO production.

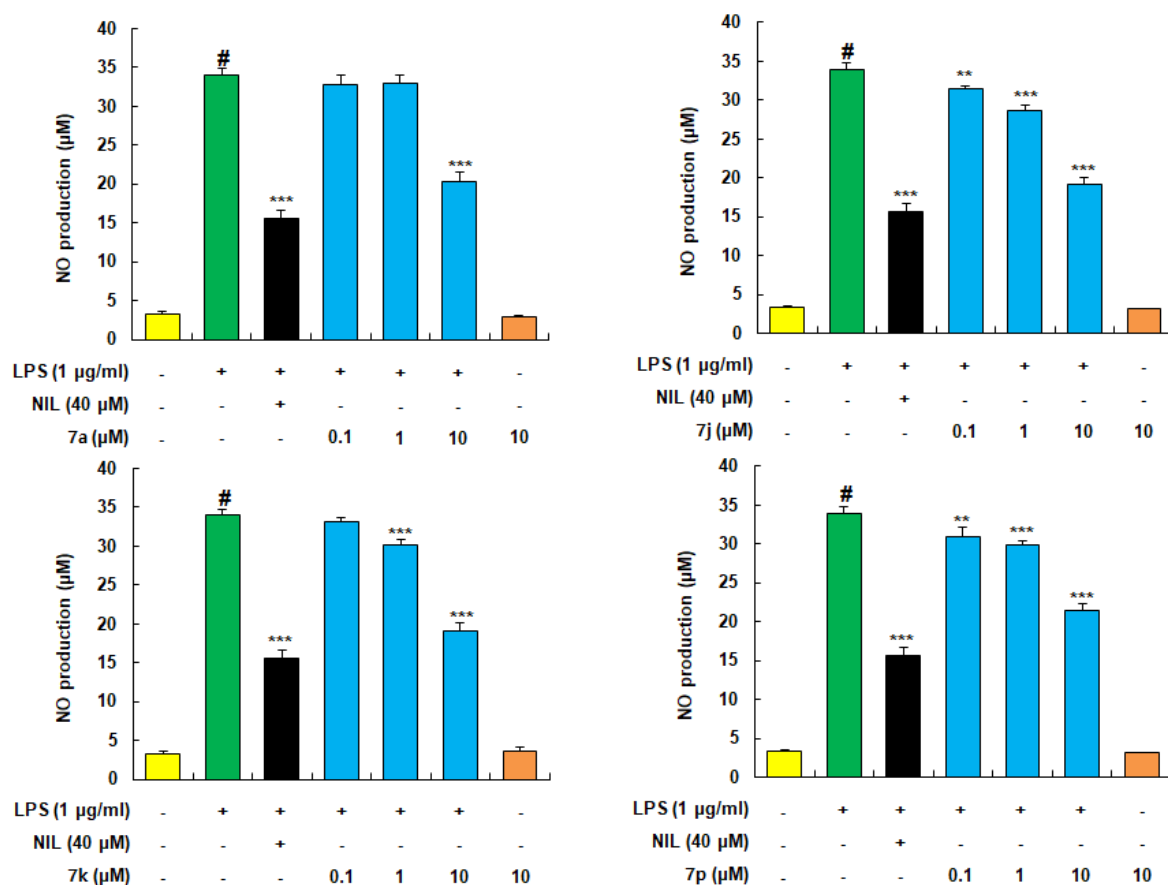


Fig. 6. Levels of NO production in RAW 264.7 macrophage cells: yellow color indicates basal NO production; dark buff color indicates NO production in non-induced cells in presence of candidate compound; green color indicates NO production in LPS-induced cells; blue color indicates NO production in LPS-induced cells in presence of candidate compounds; black color indicates NO production in LPS-induced cells in presence of standard; ** $p < 0.01$, *** $p < 0.001$.

2.2.3.4. Effect on LPS-induced PGE₂ production in RAW 264.7 macrophages

Stimulation of macrophages by LPS results in activation of mitogen-activated protein kinase (MAPK) and NF- κ B signaling pathways. Both signaling pathways lead to induction of the pro-inflammatory prostaglandin E₂ (PGE₂) production [57]. As a consequence, NF- κ B signaling pathway inhibitors would reduce PGE₂ production resulting in alleviation of inflammatory conditions. To verify the capability of the prepared IKK- β inhibitors to reduce PGE₂ production, LPS-induced RAW 264.7 macrophages model was used. As presented in Fig. 7, incubation of macrophages with candidate compounds in absence of LPS did not show significant increase in PGE₂ production indicating no inflammation stimulatory activity of

these compounds. When macrophages were incubated with LPS, PGE₂ production increased substantially from 0.16 to 33.64 ng/mL which was reduced by the standard NS-398 [58] to 12.02 ng/mL. When macrophages were incubated with LPS in the presence of 10 μM concentrations of candidate compounds, PGE₂ production decreased to 13.87, 16.53 and 19.04 ng/mL by compounds **7k**, **7a** and **7p**, respectively, while compound **7j** did not affect PGE₂ production significantly. In contrast to compounds **7j**, **7k** and **7p** whose 1 and 0.1 μM concentrations did not reduce PGE₂ production significantly, compound **7a** exhibited significant reduction of PGE₂ production even at the low 0.1 μM concentration. The calculated IC₅₀ values for inhibition of PGE₂ production by the most potent compounds **7k** and **7a** were 8.52 and 9.83 μM, respectively. These data suggest potential anti-inflammatory activity of compounds **7k** and **7a**.

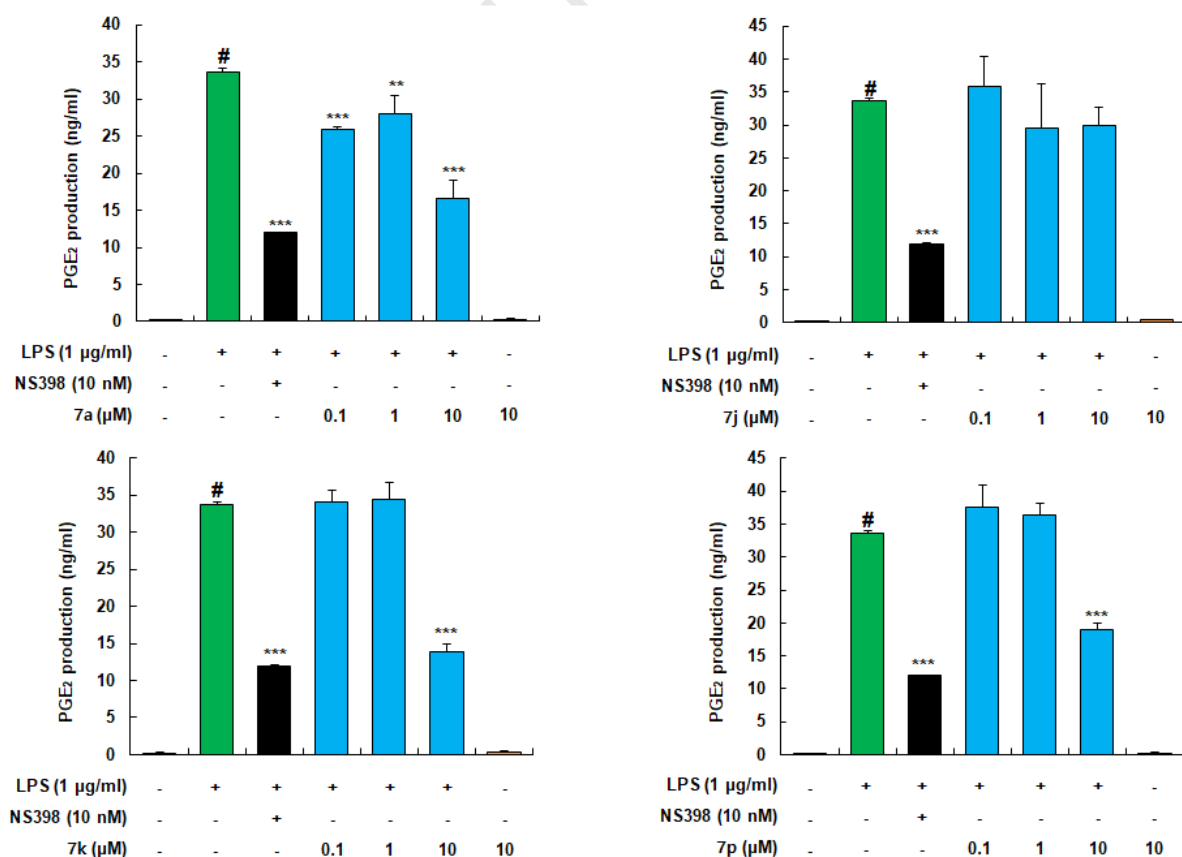


Fig. 7. Levels of PGE₂ production in LPS-induced RAW 264.7 macrophages: dark buff color indicates PGE₂

production in non-induced cells in presence of candidate compound; green color indicates PGE₂ production in LPS-induced cells; blue color indicates PGE₂ production in LPS-induced cells in presence of candidate compounds; black color indicates PGE₂ production in LPS-induced cells in presence of standard; **p<0.01, ***p<0.001.

2.2.3.5. Effect on LPS-induced IL-6 production in RAW 264.7 macrophages

Both of NF- κ B and MAPK signaling pathways are recruited in the production of IL-6 subsequent to macrophages' activation by LPS [59]. Accordingly, blockage of NF- κ B signaling *via* inhibition of IKK- β might contribute to reduction of the pro-inflammatory IL-6 production. To assess the ability of the tested compounds to reduce IL-6 production, the amounts produced of IL-6 in LPS-stimulated RAW 264.7 macrophages were determined after incubating the cells for 24 hours with LPS alone or LPS in presence of increasing concentrations of each candidate compound. As illustrated in Fig. 8, compounds **7j** and **7k** elicited a significant dose dependent reduction of IL-6 over the tested three concentrations while compound **7a** failed to show significant reduction. Although not fully comprehensible, the reduction of IL-6 production by compound **7p** was significant but the higher 10 μ M dose did not exert response higher than that of the 1 μ M dose. The high IC₅₀ values of all of the evaluated compounds might be caused by presence of LPS-stimulated signaling pathways other than NF- κ B that can contribute to production of IL-6. However, these results show that compounds **7j**, **7k** and **7p** can contribute to the reduction of IL-6 production and, hence, assist in reducing inflammation.

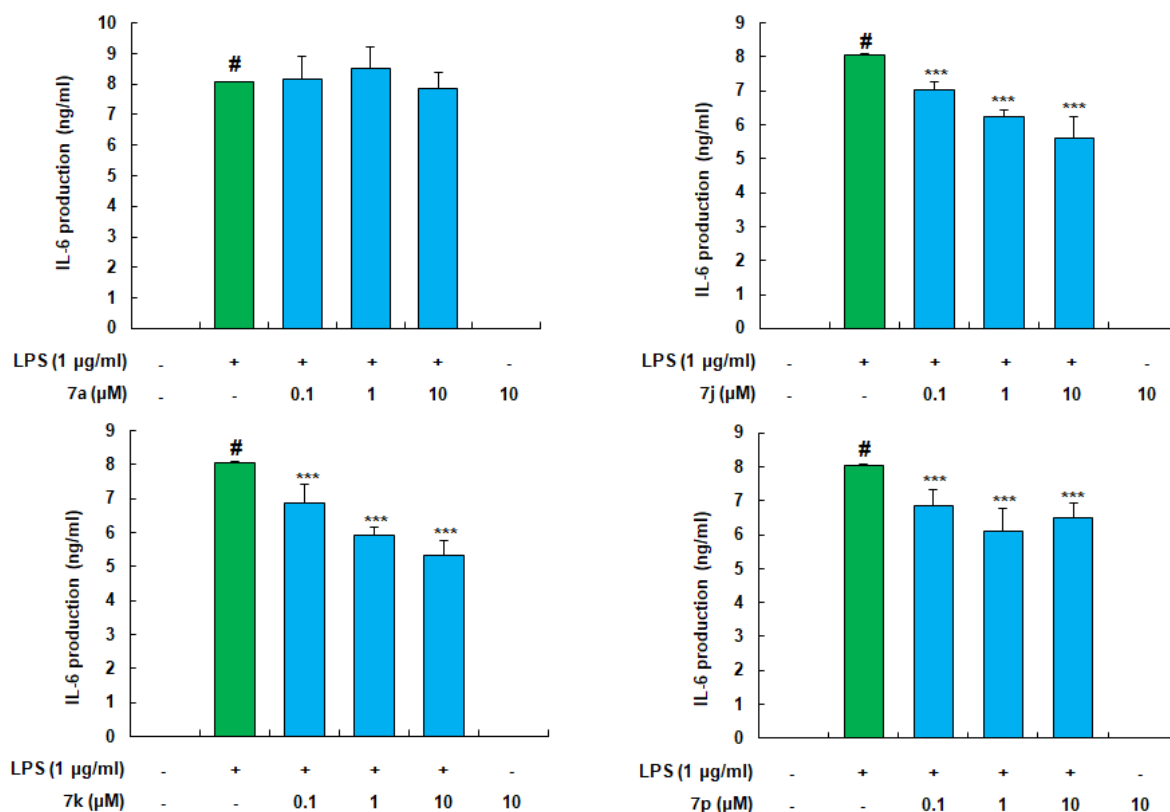


Fig. 8. Levels of IL-6 produced in RAW 264.7 macrophage cells: green color indicates presence of only LPS; blue color indicates presence of a candidate compound and LPS; *** $p < 0.001$.

In summary, the evaluation of the selected set of compounds at the cellular level revealed that they possess anti-inflammatory properties with variable capacities to reduce the production of the evaluated inflammatory mediators. While compound **7a** possessed good anti-inflammatory activity reducing the production of TNF- α , PGE₂ and NO, it did not affect the production of IL-6. On the other side, compound **7k** was less potent than **7a** in reducing TNF- α production, but it reduced the production of IL-6, PGE₂, and, NO. Although compound **7j** did not affect PGE₂ production, meanwhile, compound **7p** showed inhibition of PGE₂ production, both of them showed some inhibitory activity for the production of other evaluated inflammatory mediators.

2.2.4. Evaluation of plasma and microsomal stability

Upon *in vivo* administration, the compound stability is challenged by modification or degradation triggered by plasma enzymes and/or proteins which might lead to poor *in vivo* activity [60, 61]. The plasma instability might become a detrimental issue for the *in vivo* efficacy, especially for irreversible inhibitors [62]. Therefore, ranking compounds for *in vivo* studies should be guided by a preceded plasma stability study. Accordingly, the most potent compounds in the conducted cellular assay were subjected to evaluation of their plasma stability. In this regard, the amount remaining of compounds **7a** and **7p** after incubation with rat plasma at 37 °C were determined over a range of time intervals up to 2 hours (Fig. 9A). The obtained curve showed high plasma stability for both compounds. With 83.3% remaining after two hours, compound **7p** was slightly more stable than compounds **7a** whose remaining amount was 73.6%.

Assessment of the metabolic stability of the promising candidates is important before proceeding to *in vivo* evaluation because high metabolism rate would lead to a rapid clearance of the administered molecule and accordingly unsatisfactory circulation time within the bloodstream to elicit its action *in vivo* [60]. As hepatic microsomes are the major contributor to metabolic inactivation of drugs within the body [63], the stability of the candidate compounds **7a** and **7p** against human hepatic microsomes was assessed. In this regard, the tested compounds, as well as, mibefradil as a standard drug were incubated in a pool of human hepatic microsomes at 37 °C to determine the percent remaining at time intervals up to one hour. As presented in Fig. 9B, compound **7p** was rapidly metabolized by human hepatic microsomes with half life time around 20 min. On the other hand, compound **7a** has a lower microsomal metabolism rate comparable to the calcium channel blocker drug mibefradil. The half life time of compound **7a** was very close to one hour. Collectively, the performed plasma and microsomal stability studies present compound **7a** as a potential

candidate for *in vivo* evaluation.

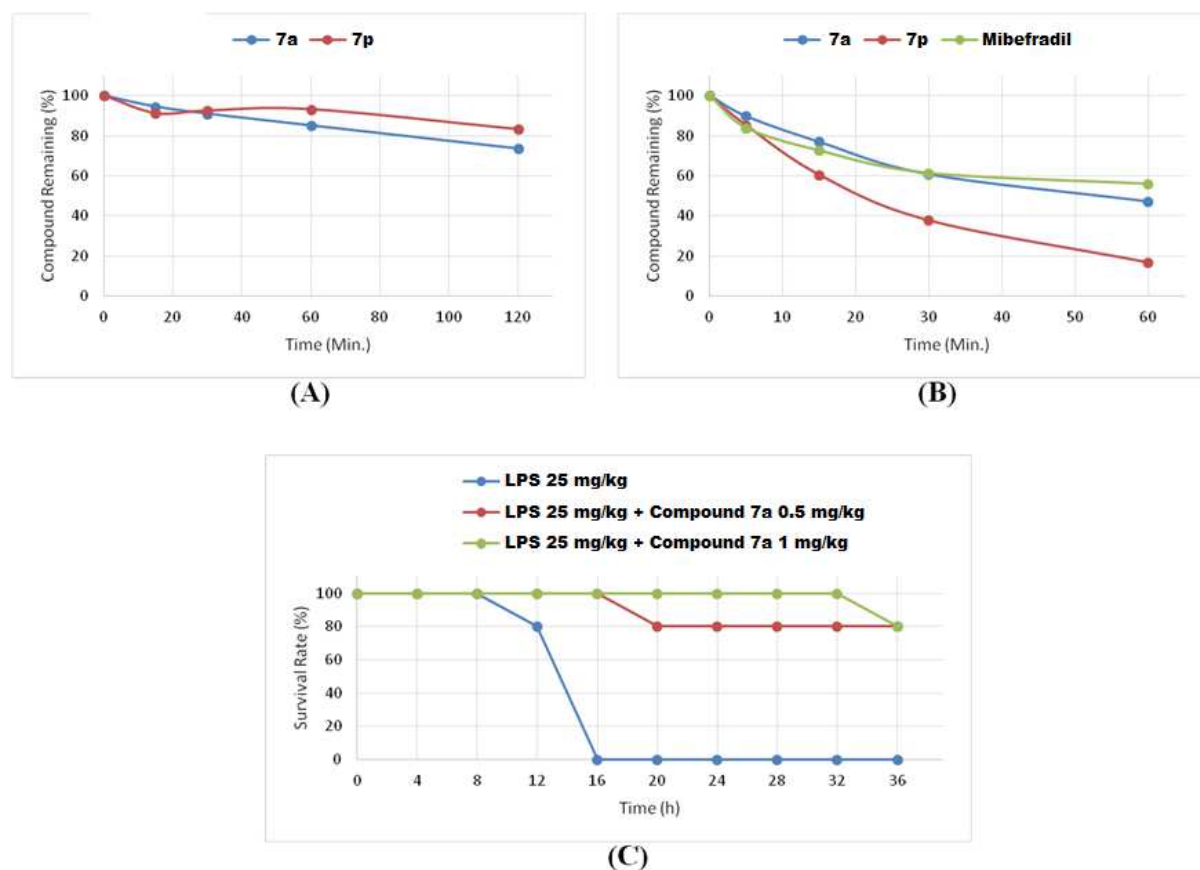


Fig. 9. (A) Plasma stability of compounds **7a** and **7p** versus time, (B) Human hepatic microsomal stability of compounds **7a** and **7p** versus time, (C) *In vivo* evaluation of compound **7a** protection against LPS-induced septic shock.

2.2.5. *In vivo* protection against septic shock

Sepsis is a systemic inflammatory response that results in the fatal septic shock. The pathogenesis of sepsis involves crucial roles for NO, PGE₂, and TNF- α [64, 65]. As compound **7a** elicited *in vitro* inhibition of LPS-induced production of the inflammatory mediators, as well as, reasonable plasma and microsomal stability, further *in vivo* assessment was conducted. The protective effect of compound **7a** against LPS-induced septic shock in mice as an animal model was assessed. As shown in Fig. 9C, compound **7a** exhibited an efficient protection at both of the two administered doses. Intraperitoneal injection of LPS

resulted in 100% mortality within 16 hours, while pre-treatment with compound **7a** resulted in survival rate of 80% at 36 hours post injection.

2.3. *In silico* simulation study

IKK- β is composed of three domains which are: the kinase domain (KD, residues 16–307), ubiquitin-like domain (ULD, residues 310–394), and scaffold dimerization domain (SDD, 410–666) 3QA8) [44]. The structure of the allosteric site allocated in the KD of IKK- β incorporates a cysteine residue (Cys46) as a part of a short loop structure connecting a short β -sheet structure (residues 41–44) with α -helix structure (residues 52–64). The literature shows that kinase activity of IKK- β is sensitive to changes at this site; mutation of Lys44 which is the last residue in the β -sheet sequence, meanwhile, is one residue away from Cys46, results in loss of IKK- β kinase activity [66]. Also, literature reports proved that the natural product covalent allosteric IKK- β inhibitor binds to Cys46 at an allosteric site [38, 39]. Previous computational study showed that blocking solvent access to Trp58 is accompanied with inhibition of kinase activity [38].

To get insights into the molecular interactions that trigger the elicited irreversible inhibition of IKK- β by the synthesized compounds, a molecular simulation study was conducted using the crystal structure of IKK- β (protein databank code: 3QA8). In this regard, covalent docking of the active compounds **7a** and **7p** was conducted using CovDock workflow as implemented in Schrödinger Suite. In such protocol, minimization of Ligand-protein complex adduct is performed after covalent docking of the ligand. The top five poses were retrieved and analyzed visually. After forming the ligand-IKK- β adduct, the top scoring pose of the active compound **7a**, possessing *para* linked *N*-methylpiperazine, showed the *N*-methylpiperazine moiety directed towards the α -helix where Trp58 is buried (Fig 10A). This

binding mode is stabilized *via* favorable hydrophobic interactions with Tyr28, Arg47, Cys46 and Arg55, anion interaction with Glu49, in addition to hydrogen bonding interaction with Pro52. Also, the second best pose of compound **7a** presented more or less similar binding mode which is stabilized by favorable hydrophobic interactions with Tyr28, Arg47 and Leu91, cation interaction with Arg55, as well as hydrogen bonding interactions with Asp90, Gln48 and Arg55 (Fig. 10B). The scores of other poses of compound **7a** were lower than these two poses. In case of analog **7p** bearing *N*-methylpiperazinyl-pentyl linked at the *meta* position, the detected binding mode showed that the *N*-methylpiperazine moiety is directed towards the α -helix in which Trp58 residue is buried which resembles the case for the active compounds bearing *p*-linked *N*-methylpiperazinyl-alkyl moiety (Fig. 10C). This binding mode is stabilized *via* a network of favorable interactions comparable to those of compounds **7a**. In lieu of these calculated binding modes, the inhibitory activity of this class of compound on IKK- β would be understandable.

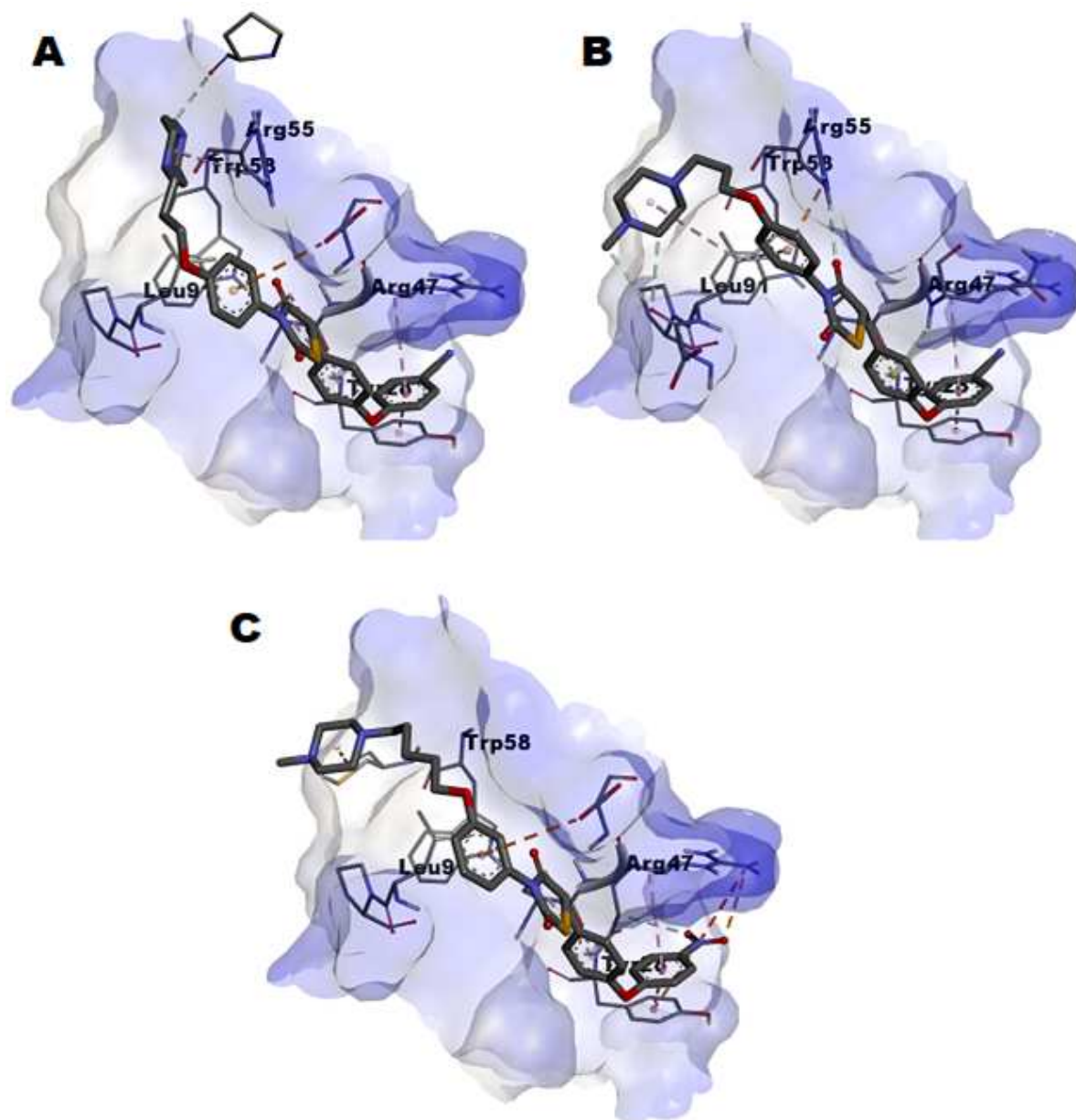


Fig. 10. The structures of covalently docked active compounds **7a** and **7p**: A) The best scoring binding mode of compound **7a**; B) The second best scoring binding mode of compound **7a**; C) The calculated binding mode for compound **7p**.

3. Conclusion

Starting from *in vitro* micromolar active lead compound **6**, a series of thiazolidine-2,4-dione derivatives was developed as irreversible allosteric covalent inhibitors of IKK- β with potential *in vivo* anti-inflammatory activity. In general, the analysis of structure activity relationship revealed that compounds possessing the *para*-attached linker were the most

potent among the prepared compounds. Almost all of them elicited submicromolar IC_{50} values with the most potent IKK- β inhibitor compound **7a** eliciting $IC_{50} = 0.20 \mu M$. In comparison, most of the derivatives having the linker attached to the *meta* position were less potent eliciting low micromolar IC_{50} values. However, when the 4-substitution on the phenoxy ring was the electron withdrawing group nitro or cyano, the IC_{50} values went again into the submicromolar range. Evaluation of the cellular activity of a set of active compounds showed that compounds **7a** and **7p** exhibited significant anti-inflammatory activity in LPS-treated macrophages through inhibition of production of inflammatory mediators. The conducted plasma and microsomal stability assays predicted superiority of *in vivo* stability of compound **7a** over **7p**. Accordingly, *in vivo* evaluation of compound **7a** was conducted in animal model of LPS-induced septic shock which confirmed its *in vivo* efficacy as it increased the survival rates of treated animal groups. *In silico* simulation study provided a reasonable explanation for the elicited IKK- β inhibitory activity. Collectively, this study indicates that the irreversible covalent allosteric IKK- β inhibitor **7a** could be a promising anti-inflammatory investigational candidate for further evaluation.

4. Experimental

4.1. Chemistry

General: All reactions and manipulations were performed using standard Schlenk techniques. All solvents and reagents have been purchased from commercial suppliers unless otherwise mentioned and used without further purification. The NMR spectra were obtained on Bruker Avance 400. 1H NMR spectra were referenced to tetramethylsilane ($\delta = 0.00$ ppm) as an internal standard and are reported as follows: chemical shift, multiplicity (br = broad, s = singlet, d = doublet, t = triplet, dd = doublet of doublet, m = multiplet). Column chromatography was performed on Merck Silica Gel 60 (230–400 mesh) and eluting solvents

for all of these chromatographic methods are noted as appropriated-mixed solvent with given volume-to-volume ratios. TLC was carried out using glass sheets pre-coated with silica gel 60 F₂₅₄ purchased by Merk. High-resolution spectra were performed on Waters ACQUITY UPLC BEH C18 1.7 μ -Q-TOF SYNAPT G2-Si High Definition Mass Spectrometry. HRMS and HPLC purity charts, preparation of 4-(3,4,5-trifluorophenoxy)benzaldehyde reagent, NMR charts as well as LC and MS conditions have been added to this article in the supplementary file. Synthesis of intermediates **9a**, **9b**, **10a**, **10b**, **11a**, **11b**, **12a** and **12b** has been reported in our recent publication [41].

4.1.1. 3-(3-(5-Iodopentyloxy)phenyl)thiazolidine-2,4-dione (12c). It has been synthesized following the same procedure used for synthesis of compounds **12a** and **12b** [41]. ¹H NMR (400 MHz, DMSO-*d*₆) δ : 1.48–1.53 (m, 2H), 1.71–1.76 (m, 2H), 1.79–1.86 (m, 2H), 3.31 (t, *J* = 6.9 Hz, 2H), 3.96 (t, *J* = 6.4 Hz, 2H), 4.29 (s, 2H), 6.84–6.87 (m, 1H), 6.90 (t, *J* = 2.0 Hz, 1H), 7.01–7.04 (m, 1H), 7.40 (t, *J* = 8.1 Hz, 1H).

4.1.2. General procedure of intermediates 13.

1-Methylpiperazine (0.15 mL, 1.34 mmol) was added to a solution of the appropriate **12** derivative (0.67 mmol) and K₂CO₃ (180 mg, 1.34 mmol) in MeCN (3 mL). The reaction mixture was stirred at room temperature for 9 h. The mixture was quenched by addition of water and extracted with DCM. The organic layer was dried over anhydrous MgSO₄, filtered and evaporated under reduced pressure. The residue was purified by column chromatography (SiO₂, DCM/MeOH = 15/1 v/v including 1% of NH₄OH).

3-(4-(3-(4-Methylpiperazin-1-yl)propoxy)phenyl)thiazolidine-2,4-dione (13a). Yield: 57%,

^1H NMR (400 MHz, DMSO- d_6) δ 1.84–1.88 (m, 2H), 2.13 (s, 3H), 2.32 (br, 8H), 2.40 (t, J = 7.1 Hz, 2H), 4.02 (t, J = 6.3 Hz, 2H), 4.27 (s, 2H), 7.02 (d, J = 8.8 Hz, 2H), 7.18 (d, J = 8.65 Hz, 2H). HRMS (ES⁺): m/z calculated for C₁₇H₂₃N₃O₃S: 350.1538 [M+H]⁺. Found 350.1540.

3-(4-(5-(4-Methylpiperazin-1-yl)pentyl)oxy)phenyl)thiazolidine-2,4-dione (13b). Yield: 43%, ^1H NMR (400 MHz, DMSO- d_6) δ 1.37–1.49 (m, 4H), 1.73 (q, J = 7.9 Hz, 2H), 2.13 (s, 3H), 2.25 (t, J = 6.7 Hz, 2H), 2.30 (br, 8H), 3.98 (t, J = 6.4 Hz, 2H), 4.27 (s, 2H), 7.02 (d, J = 8.9 Hz, 2H), 7.18 (d, J = 8.9 Hz, 2H).

3-(3-(5-(4-Methylpiperazin-1-yl)pentyl)oxy)phenyl)thiazolidine-2,4-dione (13c). Yield: 55%, ^1H NMR (400 MHz, DMSO- d_6) δ : 1.37–1.47 (m, 4H), 1.72 (t, J = 7.1 Hz, 2H), 2.13 (s, 3H), 2.23–2.33 (m, 10H), 3.95 (t, J = 6.5 Hz, 2H), 4.29 (s, 2H), 6.85 (d, J = 7.4 Hz, 1H), 6.90 (t, J = 2.0 Hz, 1H), 7.02 (dd, J = 2.3 Hz, 8.2 Hz, 1H), 7.39 (t, J = 8.1 Hz, 1H).

4.1.3. General procedure of target compounds (7a–q). NaOAc anhydrous (17.6 mg, 0.21 mmol), the appropriate aldehyde derivative (0.14 mmol) and the appropriate **13** analog (0.07 mmol) were dissolved in AcOH (3 mL) and stirred at 110 °C for 16 h. After cooling, the mixture was neutralized to pH 8 by addition of NH₄OH and extracted with DCM. The organic layer was dried over anhydrous MgSO₄, filtered and concentrated under reduced pressure. The residue was purified by column chromatography (SiO₂, DCM/MeOH = 15/1 v/v including 1% of NH₄OH).

(Z)-4-(4-((3-(4-(3-(4-Methylpiperazin-1-yl)propoxy)phenyl)-2,4-dioxothiazolidin-5-ylidene)methyl)phenoxy)benzotrile (7a). Yield: 45%, mp: 247.7–248.2 °C, HPLC purity: 8.58 min, 93.77%, ^1H NMR (400 MHz, DMSO- d_6) δ 2.28 (br, 2H), 2.84 (s, 3H), 3.60–3.79

(m, 10H), 4.14 (t, $J = 5.8$ Hz, 2H), 7.09 (d, $J = 8.7$ Hz, 2H), 7.24 (d, $J = 8.6$ Hz, 2H), 7.30 (d, $J = 8.5$ Hz, 2H), 7.37 (d, $J = 8.7$ Hz, 2H), 7.77 (d, $J = 8.6$ Hz, 2H), 7.91 (d, $J = 8.6$ Hz, 2H), 8.00 (s, 1H). ^{13}C NMR (100 MHz, DMSO- d_6) δ 23.76, 48.51, 50.04, 65.68, 106.69, 115.44, 119.09, 119.78, 120.73, 121.29, 126.19, 129.76, 129.92, 132.51, 133.00, 135.31, 157.10, 159.04, 160.23, 165.85, 167.47. HRMS (ES⁺): m/z calculated for $\text{C}_{31}\text{H}_{30}\text{N}_4\text{O}_4\text{S}$: 555.2066 [M+H]⁺. Found 555.2074.

(Z)-5-(4-(4-Fluorophenoxy)benzylidene)-3-(4-(3-(4-methylpiperazin-1-yl)propoxy)phenyl)thiazolidine-2,4-dione (7b). Yield: 38%, ^1H NMR (400 MHz, DMSO- d_6) δ 2.22 (br, 2H), 2.81 (s, 3H), 3.60–3.79 (m, 10H), 4.12 (t, $J = 5.3$ Hz, 2H), 7.08 (d, $J = 9.0$ Hz, 2H), 7.12 (d, $J = 8.8$ Hz, 2H), 7.20 (d, $J = 8.5$ Hz, 2H), 7.30 (d, $J = 8.5$ Hz, 2H), 7.36 (d, $J = 8.9$ Hz, 2H), 7.69 (d, $J = 8.9$ Hz, 2H), 7.95 (s, 1H).

(Z)-5-(4-(4-Fluorophenoxy)benzylidene)-3-(4-(5-(4-methylpiperazin-1-yl)pentyl)oxy)phenyl)thiazolidine-2,4-dione (7c). Yield: 85%, mp: 248.5–249.1 °C, HPLC purity: 8.83 min, 98.46%, ^1H NMR (400 MHz, DMSO- d_6) δ 1.47 (m, 2H), 1.76–1.77 (m, 4H), 2.81 (s, 3H), 3.30–3.44 (br, 8H), 3.59 (t, $J = 6.6$ Hz, 2H), 4.04 (t, $J = 6.1$ Hz, 2H), 7.07 (d, $J = 8.9$ Hz, 2H), 7.12 (d, $J = 8.7$ Hz, 2H), 7.19–7.22 (m, 2H), 7.29 (d, $J = 8.7$ Hz, 2H), 7.34 (d, $J = 8.9$ Hz, 2H), 7.69 (d, $J = 8.8$ Hz, 2H), 7.95 (s, 1H). ^{13}C NMR (100 MHz, DMSO- d_6) δ 23.09, 23.39, 28.46, 35.22, 42.50, 42.55, 49.66, 67.92, 115.33, 117.26, 117.50, 118.40, 120.26, 122.41, 122.49, 125.92, 128.18, 129.73, 132.78, 132.89, 151.55, 159.38, 159.83, 165.91, 167.55. HRMS (ES⁺): m/z calculated for $\text{C}_{32}\text{H}_{34}\text{FN}_3\text{O}_4\text{S}$: 576.2332 [M+H]⁺. Found 576.2319.

(Z)-5-(4-(4-Chlorophenoxy)benzylidene)-3-(4-(5-(4-methylpiperazin-1-yl)pentyl)oxy)phenyl)thiazolidine-2,4-dione (7d). Yield: 57%, mp: 272.6–273.1 °C, HPLC

purity: 9.01 min, 100%, ^1H NMR (400 MHz, DMSO- d_6) δ 1.46–1.48 (m, 2H), 1.74–1.77 (m, 4H), 2.81 (s, 3H), 3.36 (br, 8H), 3.59 (t, $J = 6.6$ Hz, 2H), 4.04 (t, $J = 6.1$ Hz, 2H), 7.07 (d, $J = 8.9$ Hz, 2H), 7.17 (d, $J = 8.9$ Hz, 4H), 7.34 (d, $J = 8.8$ Hz, 2H), 7.51 (d, $J = 8.9$ Hz, 2H), 7.71 (d, $J = 8.8$ Hz, 2H), 7.96 (s, 1H). HRMS (ES $^+$): m/z calculated for $\text{C}_{32}\text{H}_{34}\text{ClN}_3\text{O}_4\text{S}$: 592.2037 $[\text{M}+\text{H}]^+$. Found 592.2034.

(Z)-5-(4-(4-Bromophenoxy)benzylidene)-3-(4-(5-(4-methylpiperazin-1-yl)pentyl)oxy)phenyl)thiazolidine-2,4-dione (7e). Yield: 47%, mp: 276.6–278.5 °C, HPLC purity: 5.61 min, 98.73%, ^1H NMR (400 MHz, DMSO- d_6) δ 1.47–1.49 (m, 2H), 1.75–1.76 (m, 4H), 2.80 (s, 3H), 3.36 (br, 8H), 3.59 (t, $J = 5.9$ Hz, 2H), 4.05 (t, $J = 6.0$ Hz, 2H), 7.06 (d, $J = 8.9$ Hz, 2H), 7.11 (d, $J = 8.8$ Hz, 2H), 7.18 (d, $J = 8.7$ Hz, 2H), 7.34 (d, $J = 8.8$ Hz, 2H), 7.63 (d, $J = 8.7$ Hz, 2H), 7.71 (d, $J = 8.8$ Hz, 2H), 7.96 (s, 1H). HRMS (ES $^+$): m/z calculated for $\text{C}_{32}\text{H}_{34}\text{BrN}_3\text{O}_4\text{S}$: 636.1531 $[\text{M}+\text{H}]^+$. Found 636.1541.

(Z)-5-(4-(4-Methoxyphenoxy)benzylidene)-3-(4-(5-(4-methylpiperazin-1-yl)pentyl)oxy)phenyl)thiazolidine-2,4-dione (7f). Yield: 54%, ^1H NMR (400 MHz, DMSO- d_6) δ 1.47–1.49 (m, 2H), 1.74–1.77 (m, 4H), 2.85 (s, 3H), 3.35 (br, 10H), 3.77 (s, 3H), 4.03 (t, $J = 6.1$ Hz, 2H), 7.01–7.12 (m, 8H), 7.34 (d, $J = 8.9$ Hz, 2H), 7.66 (d, $J = 8.9$ Hz, 2H), 7.93 (s, 1H).

(Z)-5-(4-(4-Methylphenoxy)benzylidene)-3-(4-(5-(4-methylpiperazin-1-yl)pentyl)oxy)phenyl)thiazolidine-2,4-dione (7g). Yield: 50%, mp: 261.0–261.8 °C, HPLC purity: 5.35 min, 97.52%, ^1H NMR (400 MHz, DMSO- d_6 + D_2O) δ 1.45–1.47 (m, 2H), 1.70–1.76 (m, 5H), 2.28 (s, 3H), 2.84 (s, 3H), 3.13 (t, $J = 7.0$ Hz, 2H), 3.45 (br, 9H), 6.97 (d, $J = 7.9$ Hz, 2H), 7.05 (d, $J = 7.0$ Hz, 4H), 7.26 (t, $J = 9.3$ Hz, 4H), 7.61 (d, $J = 8.3$ Hz, 2H),

7.86 (s, 1H). ^{13}C NMR (100 MHz, DMSO- d_6 + D $_2$ O) δ 20.70, 22.85, 23.42, 28.27, 42.62, 48.37, 50.06, 67.93, 115.42, 118.30, 119.76, 120.36, 125.69, 127.67, 129.64, 131.21, 132.86, 133.27, 134.69, 152.95, 159.35, 160.08, 166.10, 167.97. HRMS (ES $^+$): m/z calculated for C $_{33}$ H $_{37}$ N $_3$ O $_4$ S: 572.2583 [M+H] $^+$. Found 572.2583.

(Z)-5-(4-(4-Aminophenoxy)benzylidene)-3-(4-(5-(4-methylpiperazin-1-

yl)pentyl)oxy)phenyl)thiazolidine-2,4-dione (7h). Yield: 48%, mp: 100.0–101.2 °C, HPLC purity: 4.11 min, 97.79%, ^1H NMR (400 MHz, DMSO- d_6) δ 1.41–1.46 (m, 4H), 1.74 (q, J = 6.5 Hz, 2H), 2.13 (s, 3H), 2.26 (t, J = 6.9 Hz, 2H), 2.35 (bs, 8H), 4.01 (t, J = 6.4 Hz, 2H), 5.09 (s, 2H), 6.62 (d, J = 6.6 Hz, 2H), 6.83 (d, J = 8.7 Hz, 2H), 7.00 (d, J = 8.8 Hz, 2H), 7.05 (d, J = 6.9 Hz, 2H), 7.32 (d, J = 8.9 Hz, 2H), 7.63 (d, J = 8.9 Hz, 2H), 7.92 (s, 1H). HRMS (ES $^+$): m/z calculated for C $_{32}$ H $_{36}$ N $_4$ O $_4$ S: 573.2535 [M+H] $^+$. Found 573.2532.

(Z)-N-(4-(4-((3-(4-((5-(4-methylpiperazin-1-yl)pentyl)oxy)phenyl)-2,4-dioxothiazolidin-5-ylidene)methyl)phenoxy)phenyl)acetamide (7i). Yield: 55%, HPLC purity: 4.47 min, 91.17%, ^1H NMR (400 MHz, DMSO- d_6) δ 1.42–1.49 (m, 4H), 1.72–1.73 (m, 2H), 2.06 (s, 3H), 2.15 (s, 3H), 2.26–2.33 (m, 10H), 4.02 (t, J = 6.4 Hz, 2H), 7.05–7.11 (m, 6H), 7.33 (d, J = 8.9 Hz, 2H), 7.67 (t, J = 9.4 Hz, 4H), 7.95 (s, 1H), 10.03 (s, 1H). ^{13}C NMR (100 MHz, DMSO- d_6) δ 23.94, 24.39, 26.47, 28.97, 46.16, 53.13, 55.19, 58.22, 68.23, 115.29, 118.18, 120.02, 120.99, 121.17, 125.86, 127.87, 129.71, 132.86, 136.75, 150.40, 159.45, 160.17, 165.92, 167.54, 168.65.

(Z)-5-(4-(4-Fluorophenoxy)benzylidene)-3-(3-((5-(4-methylpiperazin-1-

yl)pentyl)oxy)phenyl)thiazolidine-2,4-dione (7j). Yield: 44%, HPLC purity: 5.17 min, 97.11%, ^1H NMR (400 MHz, DMSO- d_6) δ 1.39–1.46 (m, 4H), 1.73 (q, J = 6.9 Hz, 2H), 2.12

(s, 3H), 2.25 (t, $J = 6.7$ Hz, 2H), 2.33 (bs, 8H), 3.97 (t, $J = 6.4$ Hz, 2H), 6.98 (d, $J = 7.9$ Hz, 1H), 7.04 (s, 1H), 7.05 (s, 1H), 7.12 (d, $J = 8.7$ Hz, 2H), 7.19 (d, $J = 6.7$ Hz, 1H), 7.21 (d, $J = 4.5$ Hz, 1H), 7.30 (t, $J = 8.8$ Hz, 2H), 7.41 (t, $J = 9.1$ Hz, 1H), 7.70 (d, $J = 8.8$ Hz, 2H), 7.96 (s, 1H). HRMS (ES⁺): m/z calculated for C₃₂H₃₄FN₃O₄S: 576.2332 [M+H]⁺. Found 576.2335.

(Z)-5-(4-(4-Chlorophenoxy)benzylidene)-3-(3-((5-(4-methylpiperazin-1-yl)pentyl)oxy)phenyl)thiazolidine-2,4-dione (7k). Yield: 60%, mp: 131.8–134.0 °C, HPLC purity: 5.39 min, 97.47%, ¹H NMR (400 MHz, DMSO-*d*₆) δ 1.41–1.47 (m, 4H), 1.74 (t, $J = 6.9$ Hz, 2H), 2.14 (s, 3H), 2.24–2.33 (m, 10H), 3.98 (t, $J = 6.4$ Hz, 2H), 6.99 (d, $J = 7.5$ Hz, 1H), 7.07 (s, 1H), 7.18 (d, $J = 8.4$ Hz, 4H), 7.43 (t, $J = 7.8$ Hz, 1H), 7.51 (d, $J = 8.8$ Hz, 2H), 7.72 (d, $J = 8.6$ Hz, 2H), 7.98 (s, 1H). HRMS (ES⁺): m/z calculated for C₃₂H₃₄ClN₃O₄S: 592.2037 [M+H]⁺. Found 592.2046.

(Z)-5-(4-(4-Bromophenoxy)benzylidene)-3-(3-((5-(4-methylpiperazin-1-yl)pentyl)oxy)phenyl)thiazolidine-2,4-dione (7l). Yield: 55%, mp: 138.8–139.7 °C, HPLC purity: 5.46 min, 90.44%, ¹H NMR (400 MHz, DMSO-*d*₆) δ 1.39–1.46 (m, 4H), 1.73 (q, $J = 6.8$ Hz, 2H), 2.12 (s, 3H), 2.25 (t, $J = 6.7$ Hz, 2H), 2.38 (bs, 8H), 3.97 (t, $J = 6.4$ Hz, 2H), 6.98 (d, $J = 8.0$ Hz, 1H), 7.05 ($J = 6.7$ Hz, 2H), 7.11 (d, $J = 8.8$ Hz, 2H), 7.18 (d, $J = 8.6$ Hz, 2H), 7.41 (t, $J = 8.6$ Hz, 1H), 7.63 (d, $J = 8.7$ Hz, 2H), 7.72 (d, $J = 8.7$ Hz, 2H), 7.97 (s, 1H). HRMS (ES⁺): m/z calculated for C₃₂H₃₄BrN₃O₄S: 636.1531 [M+H]⁺. Found 636.1531.

(Z)-5-(4-(4-Methylphenoxy)benzylidene)-3-(3-((5-(4-methylpiperazin-1-yl)pentyl)oxy)phenyl)thiazolidine-2,4-dione (7m). Yield: 49%, HPLC purity: 5.39 min, 92.61%, ¹H NMR (400 MHz, DMSO-*d*₆) δ 1.39–1.46 (m, 4H), 1.75 (q, $J = 6.5$ Hz, 2H), 2.12 (s, 3H), 2.25 (t, $J = 6.6$ Hz, 2H), 2.38 (bs, 8H), 2.39 (s, 3H), 3.97 (t, $J = 6.5$ Hz, 2H), 6.98 (d,

$J = 7.9$ Hz, 1H), 7.03–7.05 (m, 4H), 7.10 (d, $J = 8.8$ Hz, 2H), 7.27 (d, $J = 8.4$ Hz, 2H), 7.41 (t, $J = 7.8$ Hz, 1H), 7.68 (d, $J = 8.8$ Hz, 2H), 7.95 (s, 1H). HRMS (ES⁺): m/z calculated for C₃₃H₃₇N₃O₄S: 572.2583 [M+H]⁺. Found 572.2589.

(Z)-5-(4-(4-Methoxyphenoxy)benzylidene)-3-(3-((5-(4-methylpiperazin-1-yl)pentyl)oxy)phenyl)thiazolidine-2,4-dione (7n). Yield: 43%, mp: 110.0–111.6 °C, HPLC purity: 5.12 min, 95.18%, ¹H NMR (400 MHz, DMSO-*d*₆) δ 1.39–1.46 (m, 4H), 1.73 (q, $J = 7.1$ Hz, 2H), 2.12 (s, 3H), 2.25 (t, $J = 6.7$ Hz, 2H), 2.38 (bs, 8H), 3.77 (s, 3H), 3.97 (t, $J = 6.4$ Hz, 2H), 6.98 (d, $J = 7.1$ Hz, 1H), 7.01–7.07 (m, 6H), 7.11 (d, $J = 8.9$ Hz, 2H), 7.40 (t, $J = 8.9$ Hz, 1H), 7.67 (d, $J = 8.8$ Hz, 2H), 7.94 (s, 1H). HRMS (ES⁺): m/z calculated for C₃₃H₃₇N₃O₅S: 588.2532 [M+H]⁺. Found 588.2546.

(Z)-5-(4-(4-Aminophenoxy)benzylidene)-3-(3-((5-(4-methylpiperazin-1-yl)pentyl)oxy)phenyl)thiazolidine-2,4-dione (7o). Yield: 50%, ¹H NMR (400 MHz, MeOD) δ 1.39–1.46 (m, 4H), 1.73 (q, $J = 6.8$ Hz, 2H), 2.12 (s, 3H), 2.24 (t, $J = 6.8$ Hz, 2H), 2.38 (bs, 8H), 3.97 (t, $J = 6.5$ Hz, 2H), 6.62 (d, $J = 6.6$ Hz, 2H), 6.78 (d, $J = 8.8$ Hz, 2H), 6.85–6.93 (m, 5H), 7.01 (d, $J = 8.6$ Hz, 2H), 7.41 (t, $J = 8.7$ Hz, 1H), 7.57 (d, $J = 9.0$ Hz, 2H), 7.93 (s, 1H). HRMS (ES⁺): m/z calculated for C₃₂H₃₆N₄O₄S: 573.2535 [M+H]⁺. Found 573.2538.

(Z)-5-(4-(4-Nitrophenoxy)benzylidene)-3-(3-((5-(4-methylpiperazin-1-yl)pentyl)oxy)phenyl)thiazolidine-2,4-dione (7p). Yield: 56%, ¹H NMR (400 MHz, DMSO-*d*₆) δ 1.41–1.48 (m, 4H), 1.71–1.77 (m, 2H), 2.14 (s, 3H), 2.25–2.34 (m, 10H), 3.99 (t, $J = 6.4$ Hz, 2H), 7.00–7.02 (m, 1H), 7.06–7.08 (m, 2H), 7.28 (d, $J = 9.2$ Hz, 2H), 7.37 (d, $J = 8.8$ Hz, 2H), 7.44 (t, $J = 7.7$ Hz, 1H), 7.81 (d, $J = 8.8$ Hz, 2H), 8.03 (s, 1H), 8.31 (d, $J = 9.2$ Hz, 2H). ¹³C NMR (100 MHz, DMSO-*d*₆) δ 23.91, 26.47, 28.92, 46.17, 53.14, 55.20, 58.21,

68.27, 114.82, 115.89, 119.10, 120.51, 121.15, 121.54, 126.76, 130.31, 130.36, 132.51, 133.04, 134.55, 143.50, 156.83, 159.56, 162.07, 165.60, 167.15. HRMS (ES+): m/z calculated for $C_{32}H_{34}N_4O_6S$: 603.2277 $[M+H]^+$. Found 603.2287.

(Z)-5-(4-(4-Cyanophenoxy)benzylidene)-3-(3-((5-(4-methylpiperazin-1-

yl)pentyl)oxy)phenyl)thiazolidine-2,4-dione (7q). Yield: 52%, mp: 241.1–242.0 °C, HPLC purity: 4.91 min, 97.93%, 1H NMR (400 MHz, DMSO- d_6) δ 1.45–1.49 (m, 2H), 1.76–1.79 (m, 4H), 2.81 (s, 3H), 3.12 (bs, 2H), 3.63 (bs, 8H), 4.01 (t, $J = 6.2$ Hz, 2H), 7.00–7.02 (m, 1H), 7.06–7.09 (m, 2H), 7.24–7.27 (m, 2H), 7.30–7.32 (m, 2H), 7.42–7.47 (m, 1H), 7.77 (d, $J = 8.8$ Hz, 2H), 7.91 (d, $J = 8.9$ Hz, 2H), 8.01 (s, 1H). ^{13}C NMR (100 MHz, DMSO- d_6) δ 23.06, 23.39, 28.44, 48.74, 50.35, 67.94, 106.74, 114.86, 115.87, 119.05, 119.81, 120.64, 120.75, 121.28, 129.89, 130.42, 132.61, 133.02, 134.57, 135.32, 157.16, 159.47, 160.23, 165.63, 167.21. HRMS (ES+): m/z calculated for $C_{33}H_{34}N_4O_4S$: 583.2379 $[M+H]^+$. Found 583.2374.

4.2. *In vitro* IMAP[®] TR-FRET assay of IKK- β

IKK- β kinase reactions were performed in a reaction buffer (10 mM Tris-HCl, pH 7.2, 10 mM MgCl₂, 0.05% NaN₃) containing 1 mM DTT and 0.01% Tween-20 (Sigma-Aldrich) to stabilize the enzyme. The reactions were performed at room temperature for 2 h in white standard 384 plates (3572, Corning Life Sciences, Lowell, MA, USA) using 0.5 μ g/mL IKK2 (Millipore Co., Billerica, MA, USA), 1 μ M I κ B α -derived substrate (5FAMGRHDSGLDSMK-NH₂; R7574, MDS Analytical Technologies, Ontario, Canada), and 3 μ M ATP (Sigma-Aldrich). The total reaction volumes were 20 μ L, and 10 μ M compounds were pre-incubated with IKK- β enzyme for 10 min before the substrate and ATP were added. For the TR-FRET reaction, 60 μ L detection mixture (1:600 dilution of IMAP

binding reagent and 1:400 dilution of Terbium donor supplied by MDS Analytical Technologies) were added 15 h before reading the plate. The energy transfer signal was measured in a multi-label counter using the TR-FRET option (Victor II, PerkinElmer Oy, Turku, Finland). The counter setting was 340 nm excitation, 100- μ s delay, and dual-emission collection for 200 μ s at 495 and 520 nm. The energy transfer signal data were used to calculate the percentage inhibition and IC₅₀ values. The kinetic study was conducted as mentioned above using ten doses (30, 10, 3, 1, 0.3, 0.1, 0.03, 0.01, 0.003 and 0.001 μ M concentrations) of the tested compounds. However, the reactions were performed for 0, 20, 40 and 60 minutes instead of the 2 h reaction.

4.3. *In vitro* cell-based assay

4.3.1. Cell culture

RAW 264.7 macrophage cells were obtained from the Korean Cell Line Bank (Seoul, Republic of Korea). Dulbecco's modified eagle's medium (DMEM), fetal bovine serum, penicillin, and streptomycin were obtained from Life Technologies Inc. (Grand Island, NY, USA). The Raw 264.7 macrophage cells were grown at 37 °C in DMEM containing 10% fetal bovine serum, penicillin (100 units/mL) and streptomycin sulfate (100 μ g/mL) in a 5% CO₂ atmosphere.

4.3.2. Cell viability

Assay was conducted adopting MTT-cell viability protocol [3, 6, 67, 68]. Briefly, RAW 264.7 macrophage cells were seeded at 1×10^5 cells/mL in 96-well plates containing 100 μ L of DMEM medium with 10% FBS and incubated overnight. After overnight incubation, tested samples were added and the plates were incubated for 24 h. The cells were then incubated with a MTT solution [(3-(4,5-dimethylthiazol-2-yl)-2,5-diphenyltetrazolium bromide, 5

mg/mL stock solution in PBS] for 4 h at 37 °C under 5% CO₂. The medium was discarded and the formazan blue that formed in the cells was dissolved in 200 µL DMSO. Absorbance of each well was measured at 540 nm using a microplate reader (Molecular Devices Inc., CA, USA).

4.3.3. Nitrite (NO) assay

The RAW 264.7 macrophage cells were seeded in 24-well plates and incubated with samples at various concentrations or with an appropriated positive control, and then stimulated with LPS (1 µg/ml) for 24 h. Nitrite levels in culture media were determined using the Griess reaction assay and presumed to reflect NO levels. L-NIL was used for positive control.

4.3.4. PGE₂, IL-6 and TNF- α assays

Cells were plated at 2×10^5 cells/mL (RAW 264.7 macrophages) in 24-well plates and incubated overnight. Following treatment with various concentrations of samples at various concentrations or with an NS-398 (positive control) for 1 h, cells were treated with LPS (10 ng/mL) for 24 h. Dilutions of the cell culture medium were assayed for PGE₂ and TNF- α levels using a colorimetric competitive enzyme-linked immunosorbent assay (ELISA) kit (Enzo life science, NY, USA) according to the manufacturer's instructions. TNF- α and IL-6 levels in cell culture medium were quantified by ELISA using mouse DuoSet kit (R&D Systems, MN, USA) according to the manufacturer's instructions.

4.4. Plasma stability

For the evaluation of plasma stability, the tested compound (1 µM) was incubated with rat plasma at 37 °C for 0, 15, 30, 60, and 120 min. After incubation and separation treatment, the remaining compound concentration was analyzed by LC-MS/MS.

4.5. Microsomal stability

Pooled human hepatic microsomes were incubated with 0.5 mg/mL protein concentration and 1 μ M compound concentration, and metabolic stability experiments were performed. The reaction was started at 37 °C in a water bath and the reaction was terminated after 0, 5, 15, 30, 60 min and analyzed by LC-MS/MS. Compound concentrations over time were expressed as % of initial concentration.

4.6. *In vivo* evaluation

Reagents: LPS (*Salmonella enterica*, serotype enteritidis) was purchased from Sigma Chemical Co. (MO, USA).

Animals: C57BL/6 male mice (6 or 10 weeks) were obtained from Dae-Han Biolink Co. (Eumsung-Gun, Chungbuk, Republic of Korea) and maintained under constant conditions (temperature, 20–25°C; humidity, 40–60%; 12-h light/dark cycle). At 24 h before the experiment, only water was provided. All procedures were conducted in accordance with university guidelines and approved by the ethical committee for Animal Care and the Use of Laboratory Animals, College of Pharmacy, Kyung Hee University (KHP-2010-11-4).

Septic shock in mice

The septic shock model test was performed as reported previously (Chaudhry MZ, Wang JH, Blankson S, and Redmond HP (2008) Statin (cerivastatin) protects mice against sepsis-related death *via* reduced pro-inflammatory cytokines and enhanced bacterial clearance. *Surg Infect* (Larchmt)9:183–194). The C57BL/6 mice were injected intraperitoneally with PBS or LPS (25 mg/kg) dissolved in PBS. Compound **7as** (5 or 50 mg/kg) were administrated orally 1 h before LPS injection. Survival was monitored for 36 h.

4.7. Molecular modeling study

The ligands was sketched, energy minimized and prepared using tools of Schrödinger's Maestro. The crystal structure of IKK- β was retrieved from protein databank (PDB code: 3QA8). The structure was prepared using the protein preparation wizard implemented in Schrödinger. Chain A was used for performing the covalent docking study. The covalent docking procedure was performed according to covalent docking protocol without any constraint and defining Cys46 as the reactive residue in a Michael-type addition reaction. Affinity scores were calculated using Glide and the best scoring five poses were retrieved, and analyzed.

5. Conflict of Interest

Authors declare no conflict of interest.

Acknowledgement

This work was supported by the KIST Institutional programs (Grant No. 2E29260) from Korea Institute of Science and Technology and by the Creative Fusion Research Program through the Creative Allied Project funded by the National Research Council of Science & Technology (CAP-12-1-KIST).

References

- [1] M.E. Swarbrick, Chapter 3 The Learning and Evolution of Medicinal Chemistry against Kinase Targets, in: Kinase Drug Discovery, The Royal Society of Chemistry, 2012, pp. 79-95.
- [2] P. Cohen, The regulation of protein function by multisite phosphorylation – a 25 year update, Trends Biochem. Sci., 25 (2000) 596-601.
- [3] M.M. Alam, A.H.E. Hassan, K.W. Lee, M.C. Cho, J.S. Yang, J. Song, K.H. Min, J. Hong, D.H. Kim, Y.S. Lee, Design, synthesis and cytotoxicity of chimeric erlotinib-alkylphospholipid hybrids, Bioorg. Chem., 84 (2019) 51-62.

- [4] A.K. Farag, A.H.E. Hassan, H. Jeong, Y. Kwon, J.G. Choi, M.S. Oh, K.D. Park, Y.K. Kim, E.J. Roh, First-in-class DAPK1/CSF1R dual inhibitors: Discovery of 3,5-dimethoxy-N-(4-(4-methoxyphenoxy)-2-((6-morpholinopyridin-3-yl)amino)pyrimidin-5-yl)benzamide as a potential anti-tauopathies agent, *Eur. J. Med. Chem.*, 162 (2019) 161-175.
- [5] A.H.E. Hassan, S.Y. Yoo, K.W. Lee, Y.M. Yoon, H.W. Ryu, Y. Jeong, J.S. Shin, S.Y. Kang, S.Y. Kim, H.H. Lee, B.Y. Park, K.T. Lee, Y.S. Lee, Repurposing mosloflavone/5,6,7-trimethoxyflavone-resveratrol hybrids: Discovery of novel p38-alpha MAPK inhibitors as potent interceptors of macrophage-dependent production of proinflammatory mediators, *Eur. J. Med. Chem.*, 180 (2019) 253-267.
- [6] M.M. Alam, A.H.E. Hassan, Y.H. Kwon, H.J. Lee, N.Y. Kim, K.H. Min, S.Y. Lee, D.H. Kim, Y.S. Lee, Design, synthesis and evaluation of alkylphosphocholine-gefitinib conjugates as multitarget anticancer agents, *Arch. Pharm. Res.*, 41 (2018) 35-45.
- [7] A. Elkamhawy, S. Paik, A.H.E. Hassan, Y.S. Lee, E.J. Roh, Hit discovery of 4-amino-N-(4-(3-(trifluoromethyl)phenoxy)pyrimidin-5-yl)benzamide: A novel EGFR inhibitor from a designed small library, *Bioorg. Chem.*, 75 (2017) 393-405.
- [8] A.K. Farag, A. Elkamhawy, A.M. Londhe, K.T. Lee, A.N. Pae, E.J. Roh, Novel LCK/FMS inhibitors based on phenoxy pyrimidine scaffold as potential treatment for inflammatory disorders, *Eur. J. Med. Chem.*, 141 (2017) 657-675.
- [9] D. Huang, T. Zhou, K. Lafleur, C. Nevado, A. Cafilisch, Kinase selectivity potential for inhibitors targeting the ATP binding site: a network analysis, *Bioinformatics*, 26 (2010) 198-204.
- [10] Z. Fang, C. Grutter, D. Rauh, Strategies for the selective regulation of kinases with allosteric modulators: exploiting exclusive structural features, *ACS chem. Biol.*, 8 (2013) 58-70.
- [11] S. Muller, S. Knapp, CHAPTER 3 Targeting Catalytic and Non-Catalytic Functions of Protein Kinases, in: *Allosterism in Drug Discovery*, The Royal Society of Chemistry, 2017, pp. 40-64.
- [12] A.H.E. Hassan, H.R. Park, Y.M. Yoon, H.I. Kim, S.Y. Yoo, K.W. Lee, Y.S. Lee, Antiproliferative 3-deoxysphingomyelin analogs: Design, synthesis, biological evaluation and molecular docking of pyrrolidine-based 3-deoxysphingomyelin analogs as anticancer agents, *Bioorg. Chem.*, 84 (2019) 444-455.
- [13] S. De Cesco, J. Kurian, C. Dufresne, A.K. Mittermaier, N. Moitessier, Covalent inhibitors design and discovery, *Eur. J. Med. Chem.*, 138 (2017) 96-114.
- [14] A.M. Gilbert, Recent advances in irreversible kinase inhibitors, *Pharm. Pat. Anal.*, 3 (2014) 375-386.
- [15] Q. Liu, Y. Sabnis, Z. Zhao, T. Zhang, S.J. Buhrlage, L.H. Jones, N.S. Gray, Developing irreversible inhibitors of the protein kinase cysteinome, *Chem. Biol.*, 20 (2013) 146-159.
- [16] C. González-Bello, Designing Irreversible Inhibitors—Worth the Effort?, *ChemMedChem*, 11 (2016) 22-30.
- [17] K. Sanderson, Irreversible kinase inhibitors gain traction, *Nat. Rev. Drug Discov.*, 12 (2013) 649.
- [18] L. Garuti, M. Roberti, G. Bottegoni, Irreversible protein kinase inhibitors, *Curr. Med. Chem.*, 18 (2011) 2981-2994.
- [19] Z. Zhao, P.E. Bourne, Progress with covalent small-molecule kinase inhibitors, *Drug Discov.*

Today, 23 (2018) 447-453.

[20] S. Lu, J. Zhang, Designed covalent allosteric modulators: an emerging paradigm in drug discovery, *Drug Discov. Today*, 22 (2017) 447-453.

[21] J. Weisner, R. Gontla, L. van der Westhuizen, S. Oeck, J. Ketzer, P. Janning, A. Richters, T. Mühlenberg, Z. Fang, A. Taher, V. Jendrossek, S.C. Pelly, S. Bauer, W.A.L. van Otterlo, D. Rauh, Covalent-Allosteric Kinase Inhibitors, *Angew. Chem., Int. Ed.*, 54 (2015) 10313-10316.

[22] T. Liu, L. Zhang, D. Joo, S.-C. Sun, NF- κ B signaling in inflammation, *Signal Transduct. Target. Ther.*, 2 (2017) 17023.

[23] D.S. Straus, Design of small molecules targeting transcriptional activation by NF- κ B: overview of recent advances, *Expert Opin. Drug Discov.*, 4 (2009) 823-836.

[24] S.C. Gupta, C. Sundaram, S. Reuter, B.B. Aggarwal, Inhibiting NF- κ B activation by small molecules as a therapeutic strategy, *Biochim. Biophys. Acta, Gene Regul. Mech.*, 1799 (2010) 775-787.

[25] A. Elkamhawy, A.H.E. Hassan, S. Paik, Y. Sup Lee, H.H. Lee, J.S. Shin, K.T. Lee, E.J. Roh, EGFR inhibitors from cancer to inflammation: Discovery of 4-fluoro-N-(4-(3-(trifluoromethyl)phenoxy)pyrimidin-5-yl)benzamide as a novel anti-inflammatory EGFR inhibitor, *Bioorg. Chem.*, 86 (2019) 112-118.

[26] T.D. Gilmore, M. Herscovitch, Inhibitors of NF-kappaB signaling: 785 and counting, *Oncogene*, 25 (2006) 6887-6899.

[27] A.H.E. Hassan, E. Choi, Y.M. Yoon, K.W. Lee, S.Y. Yoo, M.C. Cho, J.S. Yang, H.I. Kim, J.Y. Hong, J.S. Shin, K.S. Chung, J.H. Lee, K.T. Lee, Y.S. Lee, Natural products hybrids: 3,5,4'-Trimethoxystilbene-5,6,7-trimethoxyflavone chimeric analogs as potential cytotoxic agents against diverse human cancer cells, *Eur. J. Med. Chem.*, 161 (2019) 559-580.

[28] J.A. Schmid, A. Birbach, IkappaB kinase beta (IKKbeta/IKK2/IKBKB)--a key molecule in signaling to the transcription factor NF-kappaB, *Cytokine Growth Factor Rev.*, 19 (2008) 157-165.

[29] M. Karin, Y. Yamamoto, Q.M. Wang, The IKK NF-[kappa]B system: a treasure trove for drug development, *Nat. Rev. Drug Discov.*, 3 (2004) 17-26.

[30] J.K. Durand, A.S. Baldwin, Targeting IKK and NF- κ B for Therapy, *Adv. Protein Chem. Struct. Biol.*, 107 (2017) 77-115.

[31] C. Gamble, K. McIntosh, R. Scott, K.H. Ho, R. Plevin, A. Paul, Inhibitory kappa B kinases as targets for pharmacological regulation, *Br. J. Pharmacol.*, 165 (2012) 802-819.

[32] A. Oeckinghaus, M.S. Hayden, S. Ghosh, Crosstalk in NF-[kappa]B signaling pathways, *Nat. Immunol.*, 12 (2011) 695-708.

[33] M. Hinz, C. Scheidereit, The I κ B kinase complex in NF- κ B regulation and beyond, *EMBO reports*, 15 (2014) 46-61.

[34] D.F. Lee, H.P. Kuo, C.T. Chen, J.M. Hsu, C.K. Chou, Y. Wei, H.L. Sun, L.Y. Li, B. Ping, W.C. Huang, X. He, J.Y. Hung, C.C. Lai, Q. Ding, J.L. Su, J.Y. Yang, A.A. Sahin, G.N. Hortobagyi, F.J. Tsai, C.H. Tsai, M.C. Hung, IKK beta suppression of TSC1 links inflammation and tumor angiogenesis via the mTOR pathway, *Cell*, 130 (2007) 440-455.

- [35] K. Suzuki, I.M. Verma, Phosphorylation of SNAP-23 by I κ B Kinase 2 Regulates Mast Cell Degranulation, *Cell*, 134 (2008) 485-495.
- [36] K. Ye, Inhibition of I κ B kinase in Notch signaling activates FOXO3a, *Cell Cycle*, 11 (2012) 2417-2417.
- [37] J.J. Huang, H.X. Chu, Z.Y. Jiang, X.J. Zhang, H.P. Sun, Q.D. You, Recent advances in the structure-based and ligand-based design of IKK β inhibitors as anti-inflammation and anti-cancer agents, *Curr. Med. Chem.*, 21 (2014) 3893-3917.
- [38] T. Dong, C. Li, X. Wang, L. Dian, X. Zhang, L. Li, S. Chen, R. Cao, L. Li, N. Huang, S. He, X. Lei, Ainsliadimer A selectively inhibits IKK α/β by covalently binding a conserved cysteine, *Nat. Commun.*, 6 (2015) 6522.
- [39] F. Yan, F. Yang, R. Wang, X.J. Yao, L. Bai, X. Zeng, J. Huang, V.K.W. Wong, C.W.K. Lam, H. Zhou, X. Su, J. Liu, T. Li, L. Liu, Isoliquiritigenin suppresses human T Lymphocyte activation via covalently binding cysteine 46 of I κ B kinase, *Oncotarget*, 8 (2017) 34223-34235.
- [40] H. Park, Y. Shin, H. Choe, S. Hong, Computational Design and Discovery of Nanomolar Inhibitors of I κ B Kinase β , *J. Am. Chem. Soc.*, 137 (2015) 337-348.
- [41] A. Elkamhawy, N.Y. Kim, A.H.E. Hassan, J.E. Park, J.E. Yang, K.S. Oh, B.H. Lee, M.Y. Lee, K.J. Shin, K.T. Lee, W. Hur, E.J. Roh, Design, synthesis and biological evaluation of novel thiazolidinedione derivatives as irreversible allosteric IKK- β modulators, *Eur. J. Med. Chem.*, 157 (2018) 691-704.
- [42] A. Elkamhawy, N. youn Kim, A.H.E. Hassan, J.-e. Park, J.-E. Yang, M.H. Elsherbeny, S. Paik, K.-S. Oh, B. Ho Lee, M. Young Lee, K. Jung Shin, A. Nim Pae, K.-T. Lee, E. Joo Roh, Optimization study towards more potent thiazolidine-2,4-dione IKK- β modulator: synthesis, biological evaluation and in-silico docking simulation, *Bioorg. Chem.*, (2019) 103261. <https://doi.org/10.1016/j.bioorg.2019.103261>
- [43] S. Kang, J.M. Lee, B. Jeon, A. Elkamhawy, S. Paik, J. Hong, S.J. Oh, S.H. Paek, C.J. Lee, A.H.E. Hassan, S.S. Kang, E.J. Roh, Repositioning of the antipsychotic trifluoperazine: Synthesis, biological evaluation and in silico study of trifluoperazine analogs as anti-glioblastoma agents, *Eur. J. Med. Chem.*, 151 (2018) 186-198.
- [44] G. Xu, Y.-C. Lo, Q. Li, G. Napolitano, X. Wu, X. Jiang, M. Dreano, M. Karin, H. Wu, Crystal structure of inhibitor of κ B kinase β (IKK β), *Nature*, 472 (2011) 325-330.
- [45] S. Saxena, G. Samala, J.P. Sridevi, P.B. Devi, P. Yogeewari, D. Sriram, Design and development of novel Mycobacterium tuberculosis L-alanine dehydrogenase inhibitors, *Eur. J. Med. Chem.*, 92 (2015) 401-414.
- [46] I.B. Levshin, I.V. Grigor'eva, A.A. Tsurkan, K.A. V'Yunov, A.I. Ginak, Study of azolidine reactivity and tautomerism. 53. Synthesis of 5-arylidene-2-(allylamino)- Δ 2-thiazolin-4-ones and 5-arylidene-2-imino-3-allylthiazolidin-4-ones, *Khim. Geterotsikl. Soedin.*, (1985) 494-497.
- [47] S.Q. Tang, Y.Y.I. Lee, D.S. Packiaraj, H.K. Ho, C.L.L. Chai, Systematic Evaluation of the Metabolism and Toxicity of Thiazolidinone and Imidazolidinone Heterocycles, *Chem. Res. Toxicol.*, 28 (2015) 2019-2033.
- [48] J. Yong, M.Q. Christopher, K. Silvia, V.T. Robert, Current In Vitro Kinase Assay Technologies: The

- Quest for a Universal Format, *Curr. Drug Discov. Technol.*, 5 (2008) 59-69.
- [49] S. Gul, P. Gribbon, Exemplification of the challenges associated with utilising fluorescence intensity based assays in discovery, *Expert Opin. Drug Discov.*, 5 (2010) 681-690.
- [50] R.S. Obach, R.L. Walsky, K. Venkatakrishnan, Mechanism-based inactivation of human cytochrome p450 enzymes and the prediction of drug-drug interactions, *Drug Metab. Dispos.*, 35 (2007) 246-255.
- [51] M. Fujihara, M. Muroi, K.-i. Tanamoto, T. Suzuki, H. Azuma, H. Ikeda, Molecular mechanisms of macrophage activation and deactivation by lipopolysaccharide: roles of the receptor complex, *Pharmacol. Ther.*, 100 (2003) 171-194.
- [52] F. Meng, C.A. Lowell, Lipopolysaccharide (LPS)-induced Macrophage Activation and Signal Transduction in the Absence of Src-Family Kinases Hck, Fgr, and Lyn, *J. Exp. Med.*, 185 (1997) 1661-1670.
- [53] T. van der Bruggen, S. Nijenhuis, E. van Raaij, J. Verhoef, B. Sweder van Asbeck, Lipopolysaccharide-Induced Tumor Necrosis Factor Alpha Production by Human Monocytes Involves the Raf-1/MEK1-MEK2/ERK1-ERK2 Pathway, *Infect. Immun.*, 67 (1999) 3824-3829.
- [54] L. Shi, R. Kishore, M.R. McMullen, L.E. Nagy, Lipopolysaccharide stimulation of ERK1/2 increases TNF-alpha production via Egr-1, *Am. J. Physiol. Cell Physiol.*, 282 (2002) C1205-1211.
- [55] H.J. Kim, K. Tsoyi, J.M. Heo, Y.J. Kang, M.K. Park, Y.S. Lee, J.H. Lee, H.G. Seo, H.S. Yun-Choi, K.C. Chang, Regulation of Lipopolysaccharide-Induced Inducible Nitric-Oxide Synthase Expression through the Nuclear Factor- κ B Pathway and Interferon- β /Tyrosine Kinase 2/Janus Tyrosine Kinase 2-Signal Transducer and Activator of Transcription-1 Signaling Cascades by 2-Naphthylethyl-6,7-dihydroxy-1,2,3,4-tetrahydroisoquinoline (THI 53), a New Synthetic Isoquinoline Alkaloid, *J. Pharmacol. Exp. Ther.*, 320 (2007) 782.
- [56] E.A. Hallinan, S. Tsymbalov, C.R. Dorn, B.S. Pitzele, D.W. Hansen, W.M. Moore, G.M. Jerome, J.R. Connor, L.F. Branson, D.L. Widomski, Y. Zhang, M.G. Currie, P.T. Manning, Synthesis and Biological Characterization of L-N6-(1-Iminoethyl)lysine 5-Tetrazole-amide, a Prodrug of a Selective iNOS Inhibitor, *J. Med. Chem.*, 45 (2002) 1686-1689.
- [57] Z. Yan, P.P. Stapleton, T.A. Freeman, M. Fuortes, J.M. Daly, Enhanced expression of cyclooxygenase-2 and prostaglandin E2 in response to endotoxin after trauma is dependent on MAPK and NF- κ B mechanisms, *Cellular Immunol.*, 232 (2004) 116-126.
- [58] N. Futaki, S. Takahashi, M. Yokoyama, I. Arai, S. Higuchi, S. Otomo, NS-398, a new anti-inflammatory agent, selectively inhibits prostaglandin G/H synthase/cyclooxygenase (COX-2) activity in vitro, *Prostaglandins*, 47 (1994) 55-59.
- [59] K.K. Nyati, K. Masuda, M.M. Zaman, P.K. Dubey, D. Millrine, J.P. Chalise, M. Higa, S. Li, D.M. Standley, K. Saito, H. Hanieh, T. Kishimoto, TLR4-induced NF- κ B and MAPK signaling regulate the IL-6 mRNA stabilizing protein Arid5a, *Nucleic Acids Res.*, 45 (2017) 2687-2703.
- [60] T.D.Y. Chung, D.B. Terry, L.H. Smith, In Vitro and In Vivo Assessment of ADME and PK Properties During Lead Selection and Lead Optimization – Guidelines, Benchmarks and Rules of Thumb, in: G.S. Sittampalam, N.P. Coussens, K. Brimacombe, A. Grossman, M. Arkin, D. Auld, C.

Austin, J. Baell, B. Bejcek, T.D.Y. Chung, J.L. Dahlin, V. Devanaryan, T.L. Foley, M. Glicksman, M.D. Hall, J.V. Hass, J. Inglese, P.W. Iversen, S.D. Kahl, S.C. Kales, M. Lal-Nag, Z. Li, J. McGee, O. McManus, T. Riss, O.J. Trask, Jr., J.R. Weidner, M. Xia, X. Xu (Eds.) *Assay Guidance Manual*, Eli Lilly & Company and the National Center for Advancing Translational Sciences, Bethesda (MD), 2004.

[61] L. Di, E.H. Kerns, Y. Hong, H. Chen, Development and application of high throughput plasma stability assay for drug discovery, *Int. J. Pharm.*, 297 (2005) 110-119.

[62] M.E. Prime, F.A. Brookfield, S.M. Courtney, S. Gaines, R.W. Marston, O. Ichihara, M. Li, D. Vaidya, H. Williams, A. Pedret-Dunn, L. Reed, S. Schaertl, L. Toledo-Sherman, M. Beconi, D. Macdonald, I. Muñoz-Sanjuan, C. Dominguez, J. Wityak, Irreversible 4-Aminopiperidine Transglutaminase 2 Inhibitors for Huntington's Disease, *ACS Med. Chem. Lett.*, 3 (2012) 731-735.

[63] H. Remmer, The role of the liver in drug metabolism, *Am. J. Med.*, 49 (1970) 617-629.

[64] S.M. Opal, The host response to endotoxin, antilipoplysaccharide strategies, and the management of severe sepsis, *Int. J. Med. Microbiol.*, 297 (2007) 365-377.

[65] C.A. Dinarello, Anti-Cytokine Therapies in Response to Systemic Infection, *J. Investig. Dermatol. Symp. Proc.*, 6 (2001) 244-250.

[66] J.D. Woronicz, X. Gao, Z. Cao, M. Rothe, D.V. Goeddel, I κ B Kinase- β : NF- κ B Activation and Complex Formation with I κ B Kinase- α and NIK, *Science*, 278 (1997) 866.

[67] A. Elkamhawy, J.E. Park, A.H.E. Hassan, A.N. Pae, J. Lee, B.G. Park, S. Paik, J. Do, J.H. Park, K.D. Park, B. Moon, W.K. Park, H. Cho, D.Y. Jeong, E.J. Roh, Design, synthesis, biological evaluation and molecular modelling of 2-(2-aryloxyphenyl)-1,4-dihydroisoquinolin-3(2H)-ones: A novel class of TSPO ligands modulating amyloid-beta-induced mPTP opening, *Eur. J. Pharm. Sci.*, 104 (2017) 366-381.

[68] J.-H. Won, K.-S. Chung, E.-Y. Park, J.-H. Lee, J.-H. Choi, L.A. Tapondjou, H.-J. Park, M. Nomura, A.H.E. Hassan, K.-T. Lee, 23-Hydroxyursolic Acid Isolated from the Stem Bark of *Cussonia bancoensis* Induces Apoptosis through Fas/Caspase-8-Dependent Pathway in HL-60 Human Promyelocytic Leukemia Cells, *Molecules*, 23 (2018) 3306.

Highlights

- Potent irreversible allosteric IKK- β inhibitors were developed.
- Cellular assays elucidated significant *in vitro* anti-inflammatory activity.
- *In vitro* evaluation of microsomal and plasma stabilities showed safe profile for analog **7a**.
- *In vivo* evaluation of **7a** showed its ability to protect mice against septic shock induced mortality.

Declaration of interests

The authors declare that they have no known competing financial interests or personal relationships that could have appeared to influence the work reported in this paper.

The authors declare the following financial interests/personal relationships which may be considered as potential competing interests:

Journal Pre-proof